COLLEGE OF ENGINEERING

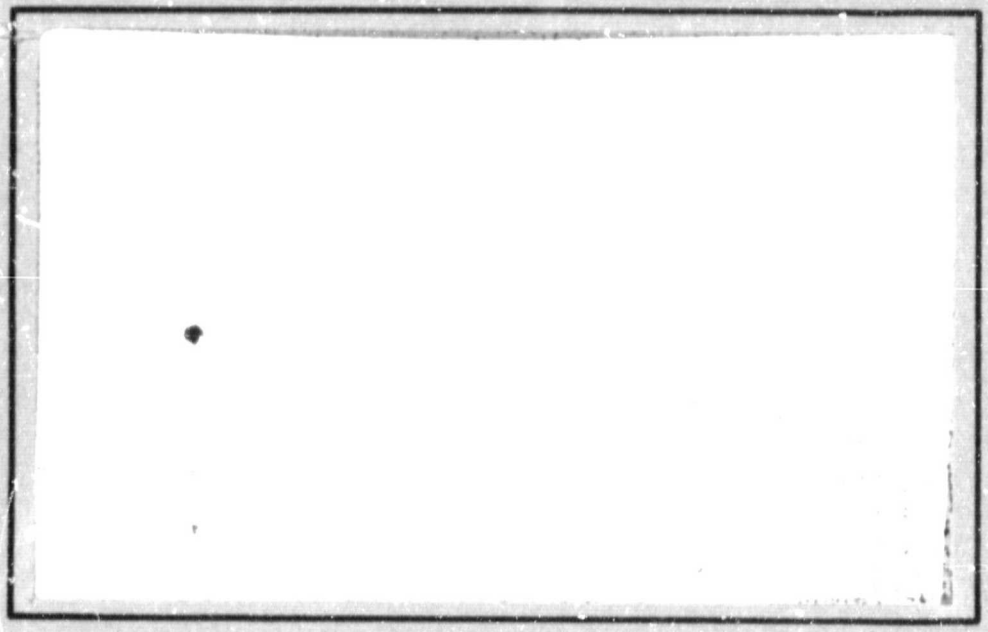

VIRGINIA POLYTECHNIC INSTITUTE AND STATE UNIVERSITY

BLACKSBURG, VIRGINIA

CLIMB-DASH REAL-TIME CALCULATIONS

A. R. Weston
P. K. A. Menon
E. M. Cliff
H. J. Kelley

July 1983

Report for the period
1 July 1982 to 30 June 1983
on research performed for
NASA Langley Research Center
under Grant NAG 1-203

Aerospace and Ocean Engineering Department
Virginia Polytechnic Institute and State University
Blacksburg, Virginia

SUMMARY

The present report consists of three AIAA papers concerning research carried out under NASA Grant NAG 1-203 during the period 1 July 1982 to 30 June 1982. Technical monitors on this research work were Dr. Douglas Price and Dr. Christopher Gracey of NASA-Langley's Theoretical Mechanics Branch. The papers are as follows:

On-Board Rear-Optimal Climb-Dash Energy Management, A. R. Weston, E. M. Cliff and H. J. Kelley, presented at the Americal Control Conference San Francisco, California, June 22-24, 1983.

Optimal Symmetric Flight with an Intermediate Vehicle Model, P. K. A. Menon, H. J. Kelley and E. M. Cliff, for presentation at the AIAA Guidance and Control Conference, Gatlinburg, Tennessee, August 15-17, 1983.

Energy State Revisited, H. J. Kelley, E. M. Cliff and A. R. Weston, for presentation at the AIAA Atmospheric Flight Mechanics Conference, Gatlinburg, Tennessee, August 15-17, 1983.

ON-BOARD NEAR-OPTIMAL CLIMB-DASH ENERGY MANAGEMENT

A. R. Weston[1]

E. M. Cliff[2]

H. J. Kelley[2]

Aerospace and Ocean Engineering Department

Virginia Polytechnic Institute and State University

Blacksburg, Virginia 24061

The subject of this paper is the study of optimal and near-optimal trajectories of high-performance fighter aircraft in symmetric flight. On-board, real-time, near-optimal guidance is considered for the climb-dash mission, using some of the boundary-layer structure and hierarchical ideas from singular perturbations. In the case of symmetric flight this resembles neighboring-optimal guidance using energy-to-go as the running variable. However, extension to 3-D flight is proposed, using families of nominal paths with heading-to-go as the additional running variable. Some computational results are presented for the symmetric case.

Introduction

On-board, real-time guidance is constrained by the limited computational resources available, particularly on fighter aircraft, where space and weight are at a premium. As a result the algorithms employed must be simple to implement and have small storage requirements. The objective of the presently described effort is to investigate practical algorithms for a variety of missions in 3-D flight. In the present paper an approach is developed for the intercept mission in symmetric flight based on a concept, sketched in Ref. 1, in which extensive numerical computation is required on the ground prior to the mission, but the on-board execution is simple. The scheme takes advantage of the boundary-layer structure common in singular perturbations, studied in Ref. (2), arising with the multiple time scales appropriate to aircraft dynamics. Energy modelling of aircraft, as first examined in Refs. (3-5) and extensively developed in Ref. (6,7) is used as the starting point for the analysis. In the symmetric case, a nominal path is generated which fairs into the dash or cruise state. Feedback coefficients are found as functions of the energy-to-go, (dash energy less actual energy), along the nominal path. These serve to generate transitions towards the nominal path, closed-loop, and to counter disturbances. In this situation the guidance method is similar to the neighboring-optimal guidance methods of Refs. (8-16). However there are two significant differences: in the present work the gain indexing is done in terms of the current energy; this avoids problems encountered in estimating the index time. Further extension to 3-D flight is considered here where families of reference paths would replace a single trajectory, with heading-to-go as the additional running variable.

Nomenclature

C_d	Drag Coefficient
C_{do}	Zero-Lift Drag Coefficient
C_ℓ	Lift Coefficient
D	Drag
E	Specific Energy
h	Altitude
L	Lift
m	Mass
Q	Fuel Flow Rate
T	Thrust
V	Velocity
x	Downrange
y	Crossrange
γ	Flight-path Angle
η	Throttle Coefficient
ϕ	Bank Angle
χ	Heading Angle
τ	Interpolation Parameter

[1] Research Associate

[2] Professor

Problem Formulation

The overall objective is to develop an on-board, real-time near-optimal flight-control system in 3-D for a variety of missions and for arbitrary initial conditions. The example developed here is for the climb-dash intercept mission in 2-D. The equations of motion for a point-mass model of an aircraft can be written:

$$\dot{E} = V(\eta T - D)/W \tag{1}$$

$$\dot{h} = V \sin\gamma \tag{2}$$

$$\dot{\gamma} = (L\cos\phi - W\cos\gamma)/mV \tag{3}$$

$$\dot{x} = V\cos\gamma \tag{4}$$

The following assumptions are embodied: fixed mass, thrust along the path, flight over a flat earth, and no winds aloft.

Aerodynamic Modelling

The aircraft which is used as an example to perform numerical calculations is a high-performance interceptor. The drag is modelled as a parabolic function of the control:

$$C_d = C_{do} + K C_\ell^2$$

The thrust is a function of Mach number and altitude; it is stored using the spline-lattice technique of Ref. 17. The flight envelope is shown in Fig. 1.

Reduced-Order Modelling

Order reduction, based on observed or assumed time-scale separations, is attractive in solving flight vehicle control problems. This is not only due to the smaller number of states and unknown initial conditions but more significantly to improvement of the conditioning of the system of differential equations by the confinement of the more unstable dynamics to

boundary-layer corrections. It has been appreciated since the work of Ref. 3 that h and γ can be changed much faster than E, which in turn is a 'fast' variable in comparison to the range. This leads to the reformulating of the equations of motion, following Ref. 6, with the interpolation parameters ε^1 and ε^2

$$\varepsilon^2 \dot{h} = V \sin\gamma \qquad (5)$$

$$\varepsilon^2 \dot{\gamma} = (L - W\cos\gamma)/mV \qquad (6)$$

$$\varepsilon^1 \dot{E} = V(\eta T - D)/W \qquad (7)$$

$$\dot{x} = V\cos\gamma \qquad (4)$$

The introduction of three separate time scales in the system must conform to the requirement of the Tihonov theory (Ref. 18) that the ratio $(\varepsilon^2/\varepsilon^1) \to 0$ as $\varepsilon^1 \to 0$, as discussed in Ref. 6. Two resulting possibilities are now discussed.

Rectilinear-Motion Model

The simplest model is found when ε^1 and ε^2 are taken as 0. The result of these assumptions on the differential equations are noted:

$$\varepsilon^1 = 0 \to \begin{bmatrix} \dot{h} = 0 \\ \dot{\gamma} = 0 \end{bmatrix} \to \begin{bmatrix} \gamma = 0 \\ L = W \end{bmatrix} \qquad (8)$$

$$(9)$$

$$\varepsilon^2 = 0 \to \dot{E} = 0 \to \eta T = D \qquad (10)$$

These equations embody the assumptions that the states h,γ, E can be varied instantly in a control-like fashion, while η and C_ℓ are chosen to satisfy (9) and (10). The control-like states h, E are chosen to minimize the Hamiltonian, $\lambda_X \dot{X}$. As λ_X is constant the min-H operation picks out the dash point on the envelope. This is the zeroth-order "outer" solution of singular-perturbation theory, which the solutions from other time scales fair into.

Energy-State Models

If $\varepsilon^1 = 1$, $\varepsilon^2 \to 0$ the next level of complexity, known as energy modelling, is found. γ and h are still assumed to be 'control-like', and 'fast', while E is now a 'slow' variable. C_ℓ is still determined by eq. (9); h and η are chosen to minimize $H = \lambda_X \dot{X} + \lambda_E \dot{E}$, where E is governed by eq. (3) and λ_E by

$$\dot{\lambda}_E = -\frac{\partial H}{\partial E} \qquad (11)$$

η and h are found in terms of the ratio of λ_E to λ_X and their signs: the ratio determines the relative importance of range rate and energy rate, while the signs determine the sense of the optimization. For example if λ_E is negative, then $\eta = 1$ minimizes H; if λ_E is positive then $\eta = 0$. If $\lambda_X = 0$ h will maximize the excess power, leading to an 'energy-climb' (Refs. 6, 19, 20); the resulting path is shown on the h-V plane in Fig. 2. This schedule shows multiple jumps in altitude which arise from realistic variations on the thrust data. This contrasts with other examples where the altitude jumps are typically due to the transonic drag-rise (Refs. 19, 20).

In the intercept problem $\lambda_X \neq 0$. The "energy climb" path traced out for $\lambda_X = 0$ is shown in Fig. 2, where the path does not fair into the "outer" solution operation at the dash point. The analysis and computations are more complex: the value of λ_E is now pivotal and the initial value of (λ_E/λ_X) will determine the ensuing path. Finding the solution which fairs into the dash-point is therefore a two-point-boundary-value problem in one dimension, solved using the usual 1-D search techniques. This 'range-optimal-energy-climb' is shown in Fig. 3, with the energy climb for comparison.

The disadvantages of this approach are that it results in a γ approximation of 0 (whereas in the climb-dash problem the actual angle for a typical high performance fighter may be in excess of 45°), and that instantaneous jumps in the altitude appear at the end-points, and also are possible during the trajectory.

Singular-Perturbation Procedure

By the use of singular-perturbation theory, boundary-layer type corrections can be used to overcome the weaknesses of the energy model, i.e. initial, internal, and final jumps in altitude. While the altitude discontinuities are eliminated by expansion to the zeroth order, nonzero γ values are obtained in the procedure of Ref. 6 by continuing the expansion to the first order. This is a nontrivial problem in the case where the altitude transitions occur at the beginning or the end of a trajectory, and is even more complex in the case of an internal altitude jump. As a result, the zeroth-order-corrected energy model loses its attraction when realistic γs are required for on-board use as commands.

On-Board Guidance

An alternative to using order reduction, suggested in Ref. (1), which is simple enough to lend itself to on-board implementation is now developed, for the case of symmetric flight. The scheme has roots in the hierarchical structure of solutions of the energy model, in which specific energy is a relatively 'slow' variable and its value determines the control-like 'fast' variables, h and γ. This suggests that trajectories of the point-mass model funnel rapidly into the vicinity of a single path, which fairs into the dash-point. The idea pursued in this and the companion paper of Ref. 1 is to determine this 'skeletal path', for the point-mass model, for as wide a range of energies as possible. This is the nominal, or reference, trajectory and the altitude and path-angle histories are recorded as functions of the energy-to-go. The next step is to generate a neighboring-optimal feedback guidance law which will control the aircraft so as to follow a neighbor of the nominal optimal path. Linear-feedback coefficients generate transients which bring the aircraft to the vicinity of the reference trajectory. The guidance law is a linear feedback control based on the difference between the nominal and actual altitude and path-angle values. The coefficients, which correspond to minimizing the second variation, as in Refs. (8 & 16), are found by perturbing the altitude and path angle separately from their nominal values along the reference trajectory. The optimal-control problem is re-solved and the partial derivative of the control with respect to the states (at fixed energy) is found in difference-quotient approximation. The C_ℓ commands which are sent to the autopilot are taken from the nominal path, with linear corrections for variation with altitude and path-angle from their nominal values:

$$C_\ell = C_\ell^*(E) + \frac{\partial C_L}{\partial h}(E)\,(h - h^*(E)) + \frac{\partial C_L}{\partial \gamma}(E)\,(\gamma - \gamma^*(E))$$

On-board use for full-throttle climb-dash requires only the storage of the states $h^*(E)$ $\gamma^*(E)$, the control $C_\ell^*(E)$, and the feedback coefficients $\frac{\partial C_L}{\partial \gamma}(E)$,

$\frac{\partial C_L}{\partial h}$ (E), as functions of the energy or energy-to-go.

Optimal Solutions Using The Point-Mass Model

A requirement of the proposed idea is a large number of optimal-control solutions to the point-mass-modelled problem. This can be done by the use of direct methods, such as gradient methods, where the control history is parameterized by sectionally-linear or spline approximation and the terminal conditions are met by either penalty or projection techniques. Alternatively the question can be posed as a two-point boundary value problem with split conditions and boundary conditions, which can be solved by indirect methods such as multiple-shooting (Refs. 21, 22). To solve the problem of time-optimal control, one forms the variational Hamiltonian:

$$H = \lambda_E \dot{E} + \lambda_h \dot{h} + \lambda_\gamma \dot{\gamma} + \lambda_x \dot{x}$$

and applies the Maximum Principle (Ref. 23, 24)). The resulting Euler differential equations are:

$$\dot{\lambda}_E = -\frac{\partial H}{\partial E}$$

$$\dot{\lambda}_h = -\frac{\partial H}{\partial h}$$

$$\dot{\lambda}_\gamma = -\frac{\partial H}{\partial \gamma}$$

$$\dot{\lambda}_x = -\frac{\partial H}{\partial x}$$

The lift and the th ottle setting must be chosen (with the present sign convention) to minimize the Hamiltonian, which requires that:

$$\frac{\partial H}{\partial C_L} = 0$$

and

$$n = 1$$

$$(\lambda_E < 0)$$

Method of Solution

Euler solutions were found in the present effort by the method of multiple shooting, using the algorithm and computer program of Refs. (14, 25) kindly supplied by DFVLR, Oberpfaffenhofen, FRG. In this method, the interval of integration is broken up into many subintervals. This is preferable to 'simple shooting', as optimization problems of lifting flight are ill-conditioned, the state-Euler system being inherently unstable. Partitioning the time interval has the effect of suppressing numerical-error growth. This need arises in the calculation of the feedback gains, found by the difference of the control at the beginning of two optimal solutions. As a result, to find the gains to 4 figures the control must be known to at least 8 figures. The multiple-shooting method has greater accuracy than the other methods available, and although it is sometimes difficult to generate the initial reference trajectory, the subsequent calculation of the feedback gains is relatively easy, as the method has good convergence properties in the vicinity of a solution.

Optimal Reference Trajectory

The first objective is to generate a reference optimal path using point-mass model dynamics, over the widest possible energy range. In the climb-dash problem being studied, the highest energy corresponds to that of the high-speed point on the aircraft envelope, the dash 'outer solution'. The lowest energy corresponds to the trajectory which just kisses the terrain limit, i.e. below this energy, optimal solutions which start at zero altitude would dive below the terrain limit if it were absent. This lower energy is found by examining the initial load factor of a family starting from level flight at the terrain limit altitude: when the initial load factor is 1, this lower energy is determined. This is shown in Fig. (4), where the initial load factor is plotted for several different initial energies. Further, as the climb is the boundary layer of the dash "outer" solution, it must fair into the dash state asymptotically. If a finite time is used, this is theoretically impossible and a final control transient is inevitable to meet the boundary conditions; however such transients can be minimized by picking a climb trajectory which is long enough in duration. A measure of smoothness with which the final approach is made is the final load factor: as the time of flight is increased it is found that the final load factor approaches a value of 1, exponentially, see Fig. 5.

A trajectory of sufficient duration that the final load factor is 1.001 is taken as the nominal path. This resembles an energy-climb schedule in that the energy of the aircraft determines the optimal altitude and path-angle; in fact the altitude chosen, for the Range-Optimal-Energy Climb is close to that from the Euler Solution at the same energy; Fig. 3 compares the two solutions in the V-h plane. It is important to note that 28-decimal-digit precision was required for successful convergence of the multiple-shooting iterative process for the "long" 2-D point-mass Euler Solutions under discussion.

Feedback Coefficients

The feedback coefficients for the neighboring-optimal guidance scheme are needed as functions of the energy-to-go along the reference path. As discussed earlier, these are found in difference-quotient approximation as the average of the forwards and backwards differences. The gains are found to be very large near the final state and the feedback system correspondingly 'nervous'. In the last foot of energy-to-go, both of the feedback gains start to grow exponentially. This sensitivity of neighboring - optimal-guidance schemes close to the terminal state has been noted in the literature (Refs. 8-16).

Simulation

Following the satisfactory splining of the nominal states, controls and feedback coefficients as functions of the energy-to-go, the guidance scheme was tested by running a simulation of the point-mass-model, using the feedback law, and comparing the resulting trajectory with an Euler solution which started from the same initial conditions. With zero disturbance the autopilot was able to follow the nominal path more than satisfactorily, over the entire range of energies, despite the inevitable errors which arise in the spline representations and numerical integration. Tests were performed with the initial altitude disturbed from that of the nominal path at different energies up to 15000 feet above and below the nominal path. The resulting trajectories are shown in Figs. 7-12. These show that the feedback law follows the optimal solution closely, even when the initial disturbance is far outside of the range of linearity of the feedback gains.

Implementation

The analysis so far has not taken into account the variation in aircraft weight, 3-D flight, winds aloft, and nonstandard atmospheric properties. The problem must be re-solved with variable weights before actual on-board use. Also, winds aloft and temperature variations could be accounted for by precomputing the variation in the stored variables using first-order approximations. A method for enhanced zeroth-order approximation via special choice of state variables is described in Ref. 26 and appears compatible with the present approach.

Conclusions

The numerical results bear out the following conclusions: first, that all trajectories which fair into the high-speed point consist of a rapid transition onto a reference or skeletal path, if they do not originate on it. Secondly, the linear-feedback scheme proposed is able to control the aircraft so that it closely follows the appropriate neighbor of the nominal path for large perturbations of initial conditions. A 3-D extension of the computational scheme is of interest in which there are two dominant states, i.e. heading-to-go in addition to energy-to-go. As a result, families of optimal paths which fair into the dash-point will be needed, and the feedback coefficients will be functions of two variables (represented via a spline lattice) instead of one.

Acknowledgments

The authors would like to thank Klaus Well, and Eugen Berger of DFVLR, Oberpfaffenhofen, West Germany, for their extensive help in the use of the multiple-shooting program which they kindly supplied. They would also like to thank Dr. C. Gracey and Dr. D. Price of NASA Langley, for their help with the numerical work performed on the NASA Langley computer. This research was supported by NASA Grant NAG-1-203, Dr. Gracey serving as technical monitor.

References

1. Kelley, H. J. and Well, K.: "An Approach to Intercept On-Board Calculations," Optimization Incorporated/DFVLR Memorandum, September 1980. An updated version appears as a 1983 ACC paper having the same title.

2. Wasow, W.: Asymptotic Expansions for Ordinary Differential Equations, Wiley/Interscience, New York, 1965.

3. Kaiser, F.;"Der Steigflug mit Strahlflugzeugen-Teil I, Bahngeschweidigbeit bosten Steigens," Versuchsbericht 262-02-L44, Messerschmitt A. G., Augsburg, April 1944, Translated as British Ministry of Supply RTP/TIB, Translation GDC/15/148T.

4. Lush, K. J.;"A review of the problem of choosing a climb technique with proposals for a new climb technique for high performance aircraft," Aero. Res. Council Rept. Memo. 2557, 1951.

5. Rutowski, E. S.; "Energy approach to the general aircraft performance problem," J. Aero. Sci., 21, 187-189, 1954.

6. Kelley, H. J.; "Aircraft maneuver optimization by reduced-order approximation," in C. T. Leondes (Ed.), Control and Dynamic Systems, Vol. X, Academic Press, New York, 1973.

7. Breakwell, J. V.; Optimal flight-path-angle translations in minimumtime airplane climbs," J. Aircraft, 14, 782-786, 1977.

8. Kelley, H. J.; "Guidance Theory and Extremal Fields," IRE Transactions on Automatic Control, Vol. 7, No. 5, 75-82, 1962.

9. Kelley, H. J.; "An Optimal Guidance Approximation Theory," IEEE Transactions on Automatic Control, Vol. 9, No. 4, 375-380, 1964.

10. Breakwell, J. V., Speyer, J. L., Bryson, A. E.; "Optimization and Control of Nonlinear Systems using the Second Variation," SIAM Control, Vol. 1, No. 2, 193-223, 1963.

11. Powers, W. F.; "A Method for Comparing Trajectories in Optimum Linear Perturbation Guidance Schemes," AIAA Journal, Vol. 6, No. 12, 2451-2452, 1968.

12. Powers, W. F.; "Techniques for Improved Convergence in Neighboring-Optimum Guidance," AIAA Journal, Vol. 8, No. 12, 2235-2341, 1970.

13. Pesch, H. J.; "Numerische Berechnung Optimaler Flugbahn Koerrekturen in Echzeit-Rechnung," Dissertation, Technische Universität München, 1978.

14. Pesch, H. J.; "Neighboring-Optimum Guidance of Space-Shuttle Orbiter-Type Vehicle," Journal of Guidance and Control, Vol. 3, No. 5, 386-392, 1980.

15. Speyer, J. L., Bryson, A. E.; "A Neighburing Optimum Feedback Law Based on Estimated Time-to-go with Application to Re-entry Flight Paths," AIAA Journal, Vol. 6, No. 5, 769-776, 1966.

16. Wood L. J.; "Perturbation Guidance for Minimum-Time Flight Paths of Spacecraft," AIAA Guidance and Control Conference, San Diego, Calif., August 9-11, 1982.

17. Mummolo, F. and Lefton, L.: "Cubic Splines and Cubic-Spline Lattices for Digital Computation," Analytical Mechanical Associates, Inc., Report No. 72-28, July 1972, revision dated December 1974.

18. Tihonov, A. N.; "Systems of Differential Equations containing Small Parameters in the Derivatives," Matematichiskii Sbornik 31, 1952.

19. Weston, A. R., Cliff, E. M., Kelley, H. J.; "Altitude Transitions in Energy Climbs," AUTOMATICA, Vol. 19, No. 2, 199-202, 1983.

20. Ardema, M. D.; "Solution of the Minimum-Time-to-Climb by Matched Asymptotic Expansions," AIAA Journal, 1976.

21. Keller, H. B.; Numerical Methods for Two-Point Boundary Value Problems, Blaisdell, London, 1968.

22. Keller, H. B.; 'Numerical Solution of Two-Point Boundary Value Problems', SIAM (CBMS-NSF), 1976.

23. Pontryagin, L. S., Boltyanskii, V. G., Gamkrelidze, R. V. and Mishchenko, E. F.; The Mathematical Theory of Optimal Processes, Wiley, New York, 1962.

24. Leitmann, G.; An Introduction to Optimal Control, McGraw-Hill, New York, 1966.

25. Bulirsh, R.; "Die Mehrztelmethode zur numerischen Losung von Nichtlinearen Randwerrproblem und Aufgaben der Optimal Steuerung," Vortrag im Lehrgang Flugbahnoptimierung der Carl-Cranz-Gesellschafte, V., October, 1971.

26. Kelley, H. J., Cliff, E. M., Weston, A. R.; "Energy State Revisited," AIAA Atmospheric Flight Mechanics Conference, Gatlinburg, Tennessee, August 15-17, 1983.

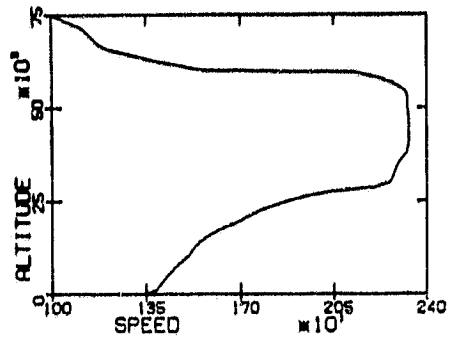

Fig. 1 Level-Flight Envelope

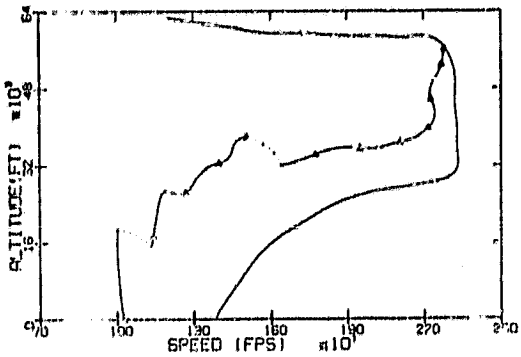

Fig. 2 Energy Climb Path in h-V Plane

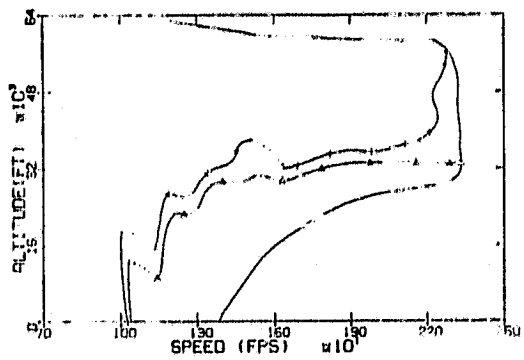

Fig. 3 Energy-Range Climb to Dash Point

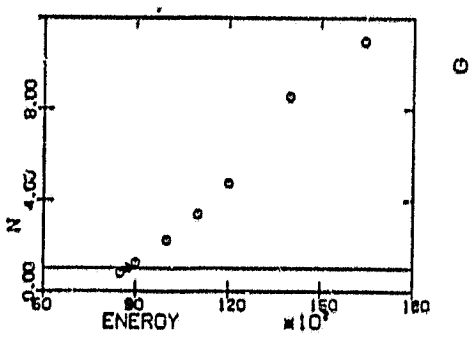

Fig. 4 Initial Load Factor vs Initial Energy

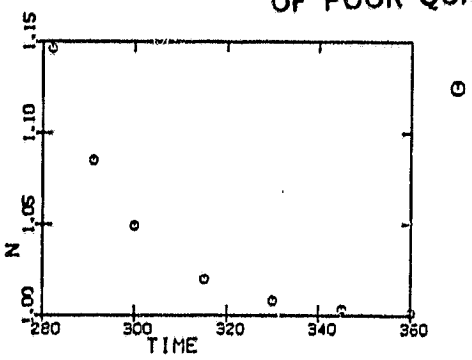

Fig. 5 Final Load Factor vs Elapsed Time

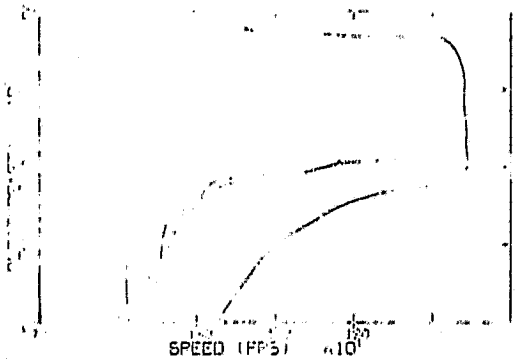

Fig. 6 Range-Energy Climb and Corresponding Point-Mass Solution

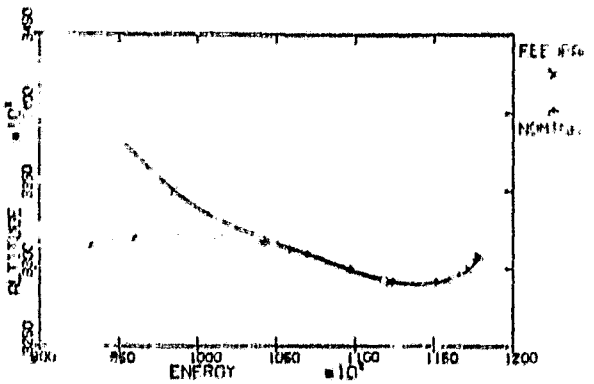

Fig. 7 Altitude vs. Energy, Initial Point 1,000 ft. above Nominal

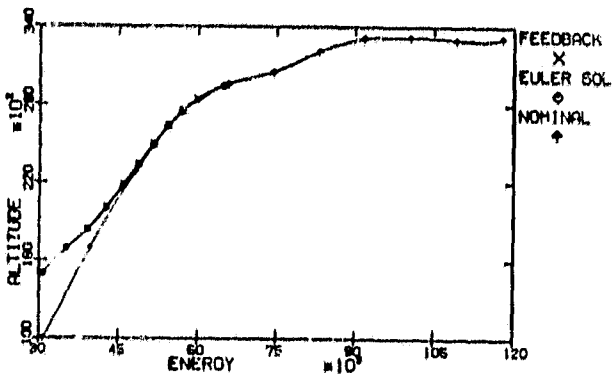

Fig. 8 Altitude vs. Energy, Initial Point 5,000 ft. above Nominal

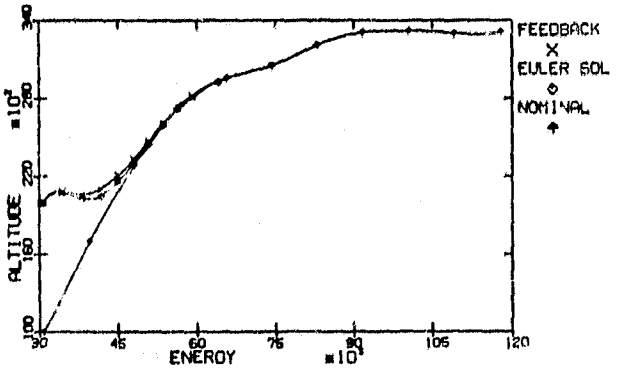

Fig. 9 Altitude vs. Energy, Initial Point10,000 ft. above Nominal

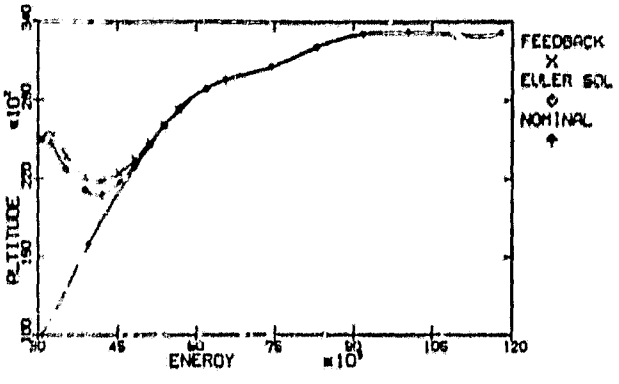

Fig. 10 Altitude vs. Energy, Initial Point15,000 ft. above Nominal

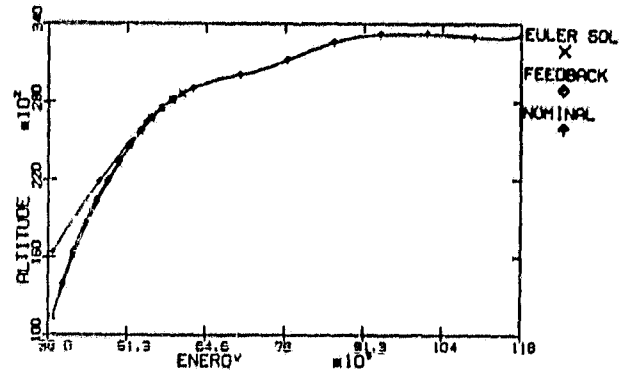

Fig. 11 Altitude vs. Energy, Initial Point 5,000 ft. below Nominal

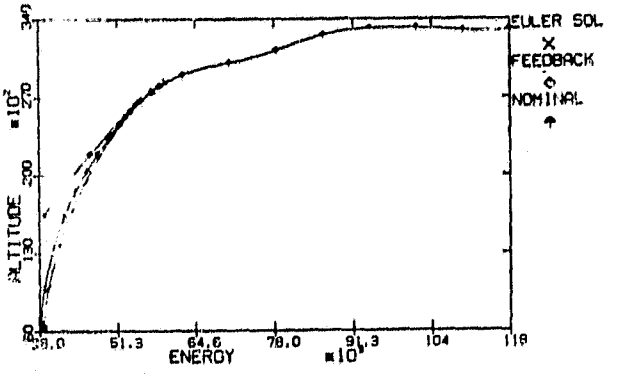

Fig. 12 Altitude vs. Energy Initial Point 10,000 ft. below Nominal

OPTIMAL SYMMETRIC FLIGHT WITH AN INTERMEDIATE VEHICLE MODEL*

P. K. A. Menon*
H. J. Kelley**
E. M. Cliff***

Virginia Polytechnic Institute and State University
Blacksburg, Virginia

Abstract

Optimal flight in the vertical plane with a vehicle model intermediate in complexity between point-mass and energy models is studied. Flight-path angle takes on the role of a control variable. Range-open problems feature subarcs of vertical flight and singular subarcs as previously studied.

The class of altitude-speed-range-time optimization problems with fuel expenditure unspecified is investigated and some interesting phenomena uncovered. The maximum-lift-to-drag glide appears as part of the family, final-time-open, with appropriate initial and terminal transient maneuvers. A family of climb-range paths appears for thrust exceeding level-flight drag, some members exhibiting oscillations. Oscillatory paths generally fail the Jacobi test for durations exceeding a period and furnish a minimum only for short-duration problems.

Minimizing paths of long duration follow a certain corridor in the V-h chart. The features of the family sharpen for the special case of thrust and drag independent of altitude, and considerable analytical attention is accorded to this for the insight it provides to the more general model.

The problem of "steepest climb" is found to be ill-posed with the vehicle model under consideration, straight-vertically-upward maneuver sequences being furnished by a family of paths alternating between upward and downward vertical flight and including a limiting "chattering" member.

Introduction

There has been interest from the beginning of optimal-flight studies in approximations featuring simplified vehicle models. Representation of drag as the drag for level flight leads to an intermediate vehicle model in which path angle γ takes on the role of a control variable and the order of the system is reduced by one. An additional order-reduction leads to an "energy-state" model with altitude or speed as a control variable (Refs. 1, 2 and 3). This is reviewed in a companion paper (Ref. 4). The present paper examines optimal symmetric flight with the intermediate vehicle model.

The analysis is based in part upon an exploration of Euler solutions for the path-angle-as-control model carried out in Ref. 5. The present analysis examines higher-order optimality conditions and "chattering-control" phenomena. The weaknesses of the model will be seen as more extensive than previously noted.

*Research supported by NASA Langley Research Center under Grant NAG 1-203
+Aerospace Engineering Graduate Student, Student Member AIAA
++Professor of Aerospace Engineering, Fellow AIAA
+++Professor of Aerospace Engineering, Member AIAA

Intermediate Vehicle Model:

The point-mass dynamical model of aircraft flight incorporating the assumption of thrust-along-the-path is given by

$$\dot{V} = g\left[\frac{(T-D)}{W} - \sin\gamma\right] \tag{1}$$

$$\dot{h} = V\sin\gamma \tag{2}$$

$$\dot{x} = V\cos\gamma \tag{3}$$

$$\dot{W} = Q \tag{4}$$

$$\dot{\gamma} = \frac{g}{V}\left(\frac{L}{W} - \cos\gamma\right) \tag{5}$$

Here V is airspeed, h altitude, x down range, W weight fuel consumed, γ flight-path angle, T thrust, D drag, g the acceleration due to gravity, L lift and Q the fuel-consumption rate.

The sweeping assumption that drag can be approximated by its level-flight value is next invoked. This permits the deletion of equation (5) and the elevation of path angle γ to control status. Lift coefficient, C_L, or angle of attack α, previously a control variable, is correspondingly assumed to be such as to satisfy (5). There is obviously trouble ahead with this modelling should γ turnout to be large in optimized maneuvering or, worse yet, should γ exhibit jump behavior.

The optimal-control problem to be treated, then, is the minimization of a function of the final values of the state variables and final time.

The variational Hamiltonian function is

$$H = \lambda_V g\left\{\frac{(T-D)}{W} - \sin\gamma\right\} + \lambda_h V\sin\gamma + \lambda_x V\cos\gamma + \lambda_W Q \tag{6}$$

and the Euler-Lagrange equations are

$$\dot{\lambda}_V = -\lambda_V \frac{g}{W}\frac{\partial}{\partial V}(T-D) - \lambda_h\sin\gamma - \lambda_x\cos\gamma - \lambda_W\frac{\partial Q}{\partial V} \tag{7}$$

$$\dot{\lambda}_h = -\lambda_V \frac{g}{W}\frac{\partial}{\partial h}(T-D) - \lambda_W\frac{\partial Q}{\partial h} \tag{8}$$

$$\dot{\lambda}_x = 0 \tag{9}$$

$$\dot{\lambda}_W = 0 \tag{10}$$

and

$$-\lambda_V g\cos\gamma + \lambda_h V\cos\gamma - \lambda_x V\sin\gamma = 0 \tag{11}$$

In the following, the time derivatives of equation (11) will be used to eliminate the time varying costates in favour of the control γ and derivatives. Note that this is somewhat formal since γ may not exist. Using equations (7) - (11) one may now proceed to eliminate those costates which are variable in the Hamiltonian. Using (11)

$$\lambda_V = \frac{V}{g}\left(\lambda_h - \lambda_x \mathrm{Tan}\gamma\right) \tag{12}$$

and hence

$$\dot{\lambda}_V = \frac{\dot{V}}{g}\left(\lambda_h - \lambda_x \mathrm{Tan}\gamma\right) + \frac{V}{g}\left(\dot{\lambda}_h - \lambda_x \dot{\gamma}\mathrm{Sec}^2\gamma\right) \tag{13}$$

substituting for $\dot{\lambda}_V$ from (12) in (8) and using equation (7)

$$\dot{\lambda}_h + \frac{V}{W}\left(\lambda_h - \lambda_x \mathrm{Tan}\gamma\right)\frac{\partial}{\partial h}(T-D) + \lambda_{\tilde{W}}\frac{\partial Q}{\partial h} = 0 \tag{14}$$

Using (13) in (7) and using equation (1), one obtains a second expression for $\dot{\lambda}_h$ as

$$\dot{\lambda}_h + \lambda_h \frac{g}{W}\left[\frac{(T-D)}{V} + \frac{\partial}{\partial V}(T-D)\right] + \lambda_x\left[\frac{g}{V\mathrm{Cos}\gamma} - \dot{\gamma}\mathrm{Sec}^2\gamma - \frac{g}{W}\mathrm{Tan}\gamma\left\{\frac{(T-D)}{V} + \frac{\partial}{\partial V}(T-D)\right\}\right] + \lambda_{\tilde{W}}\frac{g}{V}\frac{\partial Q}{\partial V} = 0 \tag{15}$$

Equations (14) and (15) may now be used to obtain an expression for λ_h in terms of λ_x and $\lambda_{\tilde{W}}$.

$$\frac{\lambda_h}{W}\left[\frac{\partial}{\partial h}V(T-D) - \frac{g}{V}\frac{\partial}{\partial V}V(T-D)\right] - \lambda_x\left[\mathrm{Tan}\gamma\left\{\frac{\partial}{\partial h}V(T-D) - \frac{g}{V}\frac{\partial}{\partial V}V(T-D)\right\} + \frac{g}{V\mathrm{Cos}\gamma} - \dot{\gamma}\mathrm{Sec}^2\gamma\right] + \lambda_{\tilde{W}}\left[\frac{\partial Q}{\partial h} - \frac{g}{V}\frac{\partial Q}{\partial V}\right] = 0 \tag{16}$$

The expressions (12) and (16) may be used for eliminating λ_V and λ_h in the Hamiltonian with the following result:

$$\mathrm{Cos}\gamma\, H\left\{\left[\frac{\partial}{\partial h} - \frac{g}{V}\frac{\partial}{\partial V}\right]\left(V(T-D)\right)\right\} - \mathrm{Cos}\gamma\,\lambda_{\tilde{W}}Q^2\left\{\left[\frac{\partial}{\partial h} - \frac{g}{V}\frac{\partial}{\partial V}\right]\left(\frac{V(T-D)}{Q}\right)^{\frac{1}{2}}\right\} - \lambda_x\left\{V^2\left[\frac{\partial}{\partial h} - \frac{g}{V}\frac{\partial}{\partial V}\right]\left((T-D)\right) - \frac{(T-D)V}{\mathrm{Cos}\gamma}\dot{\gamma}\right\} = 0 \tag{17}$$

Note that

$$\left\{\frac{\partial}{\partial h} - \frac{g}{V}\frac{\partial}{\partial V}\right\}[\ ] = \frac{\partial}{\partial h}[\ ]\Big|_{E\ =\ \mathrm{Constant}}$$

Where $E = h + \frac{V^2}{2g}$, the Specific energy.

In order to investigate the implications of this complicated expression, consider first the case of free final value of range x and fuel $\tilde{W}$. If the final values of these variables are left open, then the natural boundary conditions $\lambda_x = 0$ and $\lambda_{\tilde{W}} = 0$ apply and the optimization problem is a trade-off between final values of time t, altitude h and airspeed V, the maximum or minimum value of one of these variables or some function of these variables being sought without regard to range or fuel consumption. In equation (17), if the transversality condition for minimum time, $H = -1$ is imposed, the well-known energy-climb schedule is obtained.

One notes that, in this case, equation (17) can be satisfied either by $\cos\gamma = 0$, vertical flight, or by vanishing of the bracketed expression, viz., the partial derivative of specific excess power V(T-D) with respect to altitude with specific energy held constant. Thus the solution of this, or any, h-v-t optimum problem is made up of vertical climbs, vertical dives and "energy climbs" pieced together in the proper order. Similar considerations apply if fuel expenditure rather than time is to be minimized. In this case $H = 0$, $\lambda_x = 0$ and $\lambda_{\tilde{W}} = 1$, and equation (17) yields the minimum-fuel-climb path with fixed throttle in the V-h plane.

If range is to be maximized or minimized with final time and fuel unspecified, then $\lambda_x = \mp 1$ and $H = \lambda_{\tilde{W}} = 0$, and a first-order differential equation for path inclination emerges as follows.

$$\left\{V^2\left[\frac{\partial}{\partial h} - \frac{g}{V}\frac{\partial}{\partial V}\right](T-D) - \frac{(T-D)V\dot{\gamma}}{\mathrm{Cos}\gamma}\right\} = 0 \tag{18}$$

If one chooses $\lambda_x = -1$ and a fixed value of H (to be determined), with $\lambda_{\tilde{W}} = 0$, expression (17) is the Euler equation for maximizing range to climb with fixed final time. With $H = 0$, $\lambda_x = -1$ and a fixed value of $\lambda_{\tilde{W}}$, similarly, the maximum range to climb trajectory with fixed final value of fuel is obtained. It may be noted that the maximum range to climb problem is ill-posed in that the range to climb for thrust greater than drag without time or fuel constraints does not have a maximum or even an upper-bound. Further, fixed-throttle range-fuel trajectories are not of any significant interest in practical situations. Hence, attention will be focused on the problem of maximizing the range-to-climb with a specified final time (fixed H, $\lambda_x = -1$).

The system (1) - (3) and (18) generates a trajectory family for the range problem. The possibility of obtaining analytical solution of the system for the case of thrust and drag as arbitrary functions of altitude and air speed is remote. However, using the assumption of constant-density atmosphere, wherein the thrust and drag depend on airspeed only, one can obtain an analytical solution to this system (Ref. 5). The expression (18) can be rewritten as

$$\frac{\dot{\gamma}}{\mathrm{Cos}\gamma} = \frac{V}{(T-D)}\left\{\frac{\partial}{\partial h} - \frac{g}{V}\frac{\partial}{\partial V}\right\}(T-D) \tag{19}$$

Time may be eliminated in favor of airspeed V as an independent variable.

In the following, several transformations of independent variable are carried out without attention to monotonicity requirements, the thought being to fit the solution segments obtained into families in due course. The temptation of range as independent variable will be avoided, however, in anticipation of purely vertical motion segments. In the interest of brevity we designate $\mu \equiv (T-D)/W$

$$\frac{1}{\cos\gamma}\frac{d\gamma}{dV}(-\sin\gamma + \mu) = \frac{V}{g\mu}\left\{\frac{\partial}{\partial h} - \frac{g}{V}\frac{\partial}{\partial V}\right\}\mu \qquad (20)$$

With altitude-dependence suppressed, the path angle γ is determined as the solution of the first-order differential equation

$$\frac{1}{\cos\gamma}\frac{d\gamma}{dV}(\sin\gamma - \mu) = \frac{d\mu}{dV}\frac{1}{\mu} \qquad (21)$$

Further simplification is obtained by another change of independent variable, this time from V to μ

$$\frac{1}{\cos\gamma}\frac{d\gamma}{d\mu}(\sin\gamma - \mu) = \frac{1}{\mu} \qquad (22)$$

If the roles of independent and dependent variables are now regarded as reversed, this equation takes the form

$$\frac{d\mu}{d\gamma} + \frac{1}{\cos\gamma}\mu^2 - \mu\frac{\sin\gamma}{\cos\gamma} = 0 \qquad (23)$$

which is the form of the Bernoulli differential equation

$$\frac{d\mu}{d\gamma} + f_1(\gamma)\,\mu^2 + f_2(\gamma)\,\mu^\beta = 0 \qquad (24)$$

with $\beta = 1$. According to Kamke, (Ref. 6), this equation has the solution

$$\frac{1}{\mu} = E(\gamma)\int\frac{f_1(\gamma)}{E(\gamma)}\,d\gamma \qquad (25)$$

where

$$E(\gamma) = e^{\int f_2 d\gamma} \qquad (26)$$

with identification of f_1 and f_2 as

$$f_1(\gamma) = \frac{1}{\cos\gamma} \qquad (27)$$

$$f_2(\gamma) = -\int\frac{\sin\gamma}{\cos\gamma} \qquad (28)$$

The solution (25) becomes as follows

$$E(\gamma) = e^{-\int\frac{\sin\gamma}{\cos\gamma}d\gamma} = e^{\ln\cos\gamma} = \cos\gamma \qquad (29)$$

$$\frac{1}{\mu} = \cos\gamma\left[\int\frac{d\gamma}{\cos^2\gamma} + C\right] = \sin\gamma + C\cos\gamma \qquad (30)$$

Before expressing this relationship in the form $\gamma = \gamma(\mu)$, we relate the integration constant C to equilibrium values of μ and γ corresponding to unaccelerated flight. Such values may be designated with a superscribed bar:

$$\bar{\mu} = \sin\bar{\gamma} \qquad (31)$$

$$C = \cot\bar{\gamma} \qquad (32)$$

The solution may then be expressed as:

$$\sin\bar{\gamma}\sin\gamma + \cos\bar{\gamma}\cos\gamma = \frac{\bar{\mu}}{\mu} \qquad (33)$$

or as

$$\gamma = \bar{\gamma} + \cos^{-1}\left[\frac{\bar{\mu}}{\mu}\right] \qquad (34)$$

Here $\bar{\mu}$ is the value of μ in unaccelerated flight and

$$\bar{\gamma} = \sin^{-1}\bar{\mu} \qquad (35)$$

In Fig. 1, the solution (34) is illustrated for various values of $\bar{\mu}$. The range of angle γ has been restricted to $\pm$ 180° in this plot.

With this solution at hand, the state histories can be generated. If the thrust is taken as zero, the state-Euler system produces the flattest-glide trajectory, flown with maximum lift-to-drag ratio, along with a family of transients to and from this point (Fig. 2). When a positive margin of thrust over drag exists, a family of oscillatory solutions is generated for various values of $\bar{\mu}$ as shown in Fig. 3. It may be noted in Fig. 3 that the innermost point corresponding to $\mu = .2$ in V-γ space corresponds to flight at $(T-D)_{max}$, while along the outermost closed path, the flight path angle γ switches between $\pm$ 90°.

With the availability of the Euler solution (30) to the maximum-range problem with altitude dependence suppressed, one may proceed to obtain a similar solution to the more general Euler equation (17) using variation of parameters (Ref. 7). Equation (17) may be written as

$$\dot{\gamma} = -g\left\{\frac{\cos\gamma}{\mu}\frac{\partial\mu}{\partial V} - \cos^2\gamma\,\frac{H}{\lambda_x}\frac{1}{V^2\mu}\frac{\partial(V\mu)}{\partial V} + \cos^2\gamma\,\frac{\lambda_W}{\lambda_x}\frac{Q^2}{V^2\mu}\frac{\partial}{\partial V}\left[\frac{V\mu}{Q}\right]\right\} \qquad (36)$$

As in equation (22), the independent variable is changed from time to airspeed resulting in

$$\frac{d\gamma}{dV}(\sin\gamma - \mu) = \frac{\cos\gamma}{\mu}\frac{d\mu}{dV} - \cos^2\gamma\,\frac{H}{\lambda_x}\frac{1}{V^2\mu}\frac{d}{dV}(V\mu) + \cos^2\gamma\,\frac{\lambda_W}{\lambda_x}\frac{Q^2}{V^2\mu}\frac{d}{dV}\left[\frac{V\mu}{Q}\right] \qquad (37)$$

Rearranging, one obtains

$$\frac{d\gamma}{dV}(\sin\gamma - \mu) - \frac{\cos\gamma}{\mu}\frac{\partial\mu}{\partial V} = -\cos^2\gamma\,\frac{H}{\lambda_x}\frac{1}{V^2\mu}\frac{d}{dV}(V\mu) + \cos^2\gamma\,\frac{\lambda_W}{\lambda_x}\frac{Q^2}{V^2\mu}\frac{d}{dV}\left[\frac{V\mu}{Q}\right] \qquad (38)$$

Equation (30) is the analytical solution to the differential equation (38) with H and λ_W both zero. The expression (30) may be differentiated with respect to airspeed to obtain

$$-\frac{1}{\mu^2}\frac{\partial\mu}{\partial V} = (\cos\gamma - C\sin\gamma)\frac{d\gamma}{dV} + \frac{dC}{dV}\cos\gamma \qquad (39)$$

Note here that C is no longer a constant, but a function of the independent variable V. Substituting for μ in (39) from (30)

$$\frac{1}{\mu}\frac{\partial \mu}{\partial V} = -\frac{\left[(\cos\gamma - C\sin\gamma)\frac{d\gamma}{dV} + \frac{dc}{dV}\cos\gamma\right]}{(\sin\gamma + C\cos\gamma)} \quad (40)$$

Using equation (40) in (38)

$$\frac{\cos^2\gamma}{\sin\gamma + C\cos\gamma}\frac{dC}{dV} = -\cos^2\gamma\,\frac{H}{\lambda_x}\frac{1}{V^2\mu}\frac{d}{dV}(V\mu) + \cos^2\gamma\,\frac{\lambda_W}{\lambda_x}\cdot\frac{Q^2}{V^2\mu}\frac{d}{dV}\left[\frac{V\mu}{Q}\right] \quad (41)$$

Since $\mu = \frac{1}{\sin\gamma + C\cos\gamma}$ from (30),

$$\cos^2\gamma\frac{dC}{dV} = \cos^2\gamma\left[-\frac{H}{\lambda_x}\left\{\frac{1}{V^2\mu} + \frac{1}{V\mu^2}\frac{d\mu}{dV}\right\} + \frac{\lambda_W}{\lambda_x}\left\{\frac{Q}{V^2\mu} + \frac{Q}{V\mu^2}\frac{d\mu}{dV} - \frac{1}{V\mu}\frac{dQ}{dV}\right\}\right] \quad (42)$$

The quantities within the $\{\ \}$ brackets can be identified as

$$-\frac{d}{dV}\left[\frac{1}{V\mu}\right] = \frac{1}{V^2\mu} + \frac{1}{V\mu^2}\frac{d\mu}{dV} \quad (43)$$

and

$$-\frac{d}{dV}\left[\frac{Q}{V\mu}\right] = -\frac{1}{V\mu}\frac{dQ}{dV} + \frac{1}{V\mu^2}\frac{d\mu}{dV} + \frac{Q}{V^2\mu} \quad (44)$$

From which

$$\frac{dC}{dV} = \frac{H}{\lambda_x}\frac{d}{dV}\left[\frac{1}{V\mu}\right] - \frac{\lambda_W}{\lambda_x}\frac{d}{dV}\left[\frac{Q}{V\mu}\right] \quad (45)$$

Equation (45) is readily integrated to yield

$$C = \frac{H}{\lambda_x}\frac{1}{V\mu} - \frac{\lambda_W}{\lambda_x}\frac{Q}{V\mu} + C_1 \quad (46)$$

where C_1 is an arbitrary constant. Hence for the time-range-fuel problem, the solution with altitude dependence suppressed is

$$\frac{1}{\mu} = \sin\gamma + \left(\frac{H}{\lambda_x} - \frac{\lambda_W}{\lambda_x}\frac{Q}{V\mu} + C_1\right)\cos\gamma \quad (47)$$

To express the above result in the form $\gamma = \gamma(\mu)$, we need to relate the integration constant c_1 to equilibrium values of μ and γ corresponding to unaccelerated flight. Unlike the situation in the simpler problem, the interpretation of equation (47) is not straight forward.

From a practical viewpoint the time-range problem is of main interest since minimum-fuel problems with fixed throttle are rare. Fuel-range problem will not be discussed further in the present paper and in subsequent development the fuel multiplier λ_W will be taken as zero.

Investigation of equilibrium points with $\lambda_W = 0$ results in a plot of the values of H/λ_x vs airspeed as shown in Fig. 4 for a parabolic (T-D) distribution illustrated in Fig. 5. In Fig. 4 three separate regimes can be identified. H/λ_x values to the left of the $(T-D)_{max}$ velocity are positive while those between the $(T-D)_{max}$ point and the $V(T-D)_{max}$ point have a negative sign. All H/λ_x values to the right of the speed for $V(T-D)_{max}$ are positive. Any of these values may be used to evaluate the arbitrary constant c_1 as follows. As in (31)

$$\bar{\mu} = \sin\bar{\gamma} \quad (48)$$

$$\bar{V} = V\Big|_{\text{Equilibrium value of } \frac{H}{\lambda_x}} \quad (49)$$

$$\cot\bar{\gamma} = \frac{H}{\lambda_x}\frac{1}{\bar{V}\bar{\mu}} + C_1 \quad (50)$$

or

$$C_1 = \cot\bar{\gamma} - \frac{H}{\lambda_x}\frac{1}{\bar{V}\bar{\mu}} \quad (51)$$

using (51) in (47)

$$\frac{1}{\mu} = \sin\gamma + \left[\frac{H}{\lambda_x}\left\{\frac{1}{V\mu} - \frac{1}{\bar{V}\bar{\mu}}\right\} + \cot\bar{\gamma}\right]\cos\gamma \quad (52)$$

putting $\Delta = \left[\frac{H}{\lambda_x}\left\{\frac{1}{V\mu} - \frac{1}{\bar{V}\bar{\mu}}\right\} + \cot\bar{\gamma}\right]$ and using a well known Trignometric identity,

$$\gamma = \tan^{-1}\left[\frac{1}{\Delta}\right] + \cos^{-1}\left[\frac{1}{\mu\sqrt{\Delta^2+1}}\right] \quad (53)$$

Equation (53) is the Euler solution to the time-range problem with altitude dependence of μ suppressed. In Figs. 6, 7 and 8, the analytical solution evaluated for representative H/λ_x values from each of the three regimes is shown. Fig. 6 and 7 indicate oscillatory solutions and are in the neighborhood of a stable equilibrium point. The similarity of these figures to Fig. 3 is striking. The solutions in Fig. 8 are non-oscillatory and bear some resemblance to Fig. 2.

Summarizing, one notes that the range problem has oscillatory solutions when a positive margin of thrust over drag exists. With zero thrust the solution obtained is the flattest glide with a family of transients to and from the maximum lift-to-drag point. For the time-range problem, values of H/λ_x to the left (low speed end) of the $V(T-D)_{max}$ point produce oscillatory solution while on the right of the $V(T-D)_{max}$ point a family of transients to and from the equilibrium point defined by the choice of H/λ_x is obtained.

Legendre-Clebsch necessary condition:

From the Euler-Lagrange equations, with $\lambda_W = 0$

$$\frac{\partial H}{\partial\gamma} = -\lambda_V g\cos\gamma + \lambda_h V\cos\gamma - \lambda_x V\sin\gamma \quad (54)$$

and

$$\frac{\partial^2 H}{\partial\gamma^2} = (\lambda_V g - \lambda_h V)\sin\gamma - \lambda_x V\cos\gamma \quad (55)$$

Setting the left-hand side of equation (54) to zero as required for a stationary minimum of H leads to

$$\tan\gamma = \frac{\lambda_h V - \lambda_V g}{\lambda_x V} \text{ or } \frac{\lambda_V g - \lambda_h V}{-\lambda_x V} \quad (56)$$

From (56), then $\sin\gamma = \frac{(\lambda_h V - \lambda_V g)\sigma}{\sqrt{(\lambda_h V - \lambda_V g)^2 + \lambda_x^2 V^2}}$ (57)

and

$$\text{Cos}\gamma = \frac{\lambda_x V \sigma}{\sqrt{(\lambda_h V - \lambda_V g)^2 + \lambda_x^2 V^2}} \qquad (58)$$

where $\sigma = \pm 1$

Using (57) and (58) in (55), it is possible to determine σ.

Next, one may employ the transversality conditions for the range problem, viz. $\lambda_x = 1$ for range minimization and $\lambda_x = -1$ for range maximization. These lead to

$$\lambda_x = 1, \frac{\partial^2 H}{\partial \gamma^2} > 0 \quad \text{if } \gamma \text{ lies in the second or third quadrant} \qquad (59)$$

$$\lambda_x = -1, \frac{\partial^2 H}{\partial \gamma^2} < 0 \quad \text{if } \gamma \text{ lies in the first or fourth quadrant} \qquad (60)$$

It is apparent that with no restrictions on the path inclination, the minimum-range trajectory is that which maximizes the range in the negative direction. If one imposes an artificial limit on the path angle γ, say $-90 \leq \gamma \leq +90$, the minimum-range trajectories are vertical up-down flight segments and any (V,h) pair can be reached in zero range if there exists a positive margin of thrust over drag. Thus, with the vehicle model considered, there is no limit to the steepness of climb.

The Legendre-Clebsch necessary conditions are met in strengthened form for the maximum-range problem for values of the path angle γ in the first or fourth quadrants. However, physical reasoning makes clear that a range maximization problem without time or fuel constraints will not possess a proper maximum or even an upper bound. In view of the above, the problem of interest is to maximize the range to climb from an initial (V,h) pair to a final (V,h) pair in a fixed time. This problem is of value in studies of the type reported in Ref. 8 for a point-mass-modelled vehicle.

It may be noted at this point that in the cases of time and/or fuel minimization problems with range open, the Legendre-Clebsch necessary condition is met only in weak form along central arcs and, hence, these trajectories fall into the class of singular extremals.

Conjugate-point test:

The Legendre-Clebsch necessary condition is met with a margin for the time-range problem and hence the Euler solution (17) with $\lambda_W = 0$ furnishes a relative minimum for initial and terminal points sufficiently close together. For extremals of finite length, however, the task of ensuring that the second variation is non-negative for admissible neighboring paths leads to the accessory-minimum problem in the calculus of variations. This in essence boils down to a search for a system of admissible variations, not identically zero, which offer the most severe competition in the sense of minimizing the second variation. If a system of nonzero variations can be found which makes the second variation zero, then it is clear that a neighboring path is competitive and that the test extremal furnishes at best an improper minimum and at worst a merely stationary value (Ref. 9). The first value of the independent variable $x = x^* > x_0$ for which such a nontrivial system can be found defines a conjugate point.

Following the analysis of Ref. 9 for the Mayer problem, the rank of the matrix of variations of states and the multiplier corresponding to the state being minimized with respect to the initial values of costates is evaluated along the test extremal, viz.

$$\text{The rank of } \begin{bmatrix} \frac{\partial x_2}{\partial \lambda_1}_0 & \frac{\partial x_2}{\partial \lambda_2}_0 & \cdots & \frac{\partial x_2}{\partial \lambda_n}_0 \\ \vdots & \vdots & & \vdots \\ \frac{\partial x_n}{\partial \lambda_1}_0 & \frac{\partial x_n}{\partial \lambda_2}_0 & \cdots & \frac{\partial x_n}{\partial \lambda_n}_0 \\ \frac{\partial \lambda_1}{\partial \lambda_1}_0 & \frac{\partial \lambda_1}{\partial \lambda_2}_0 & \cdots & \frac{\partial \lambda_1}{\partial \lambda_n}_0 \end{bmatrix} \qquad (61)$$

provides the criterion for the existence of a conjugate point. If the rank of the test matrix (61) drops at any point along the test extremal, it is indicative of the occurrence of a conjugate point.

For the time-range problem, if the independent variable is changed from time to range, the equations of motion become

$$h' = \text{Tan}\gamma \qquad (62)$$

$$V' = \frac{g(T-D)}{WV\,\text{Cos}\gamma} - \frac{g}{V}\text{Tan}\gamma \qquad (63)$$

The optimal-control problem then is to maximize the final value of altitude 'h' for a specified range with time fixed. With the interpretation of H as the time multiplier, the test matrix (61) becomes

$$\begin{bmatrix} \frac{\partial V}{\partial \lambda_h}_0 & \frac{\partial V}{\partial H}_0 & \frac{\partial V}{\partial \gamma}_0 \\ \frac{\partial t}{\partial \lambda_h}_0 & \frac{\partial t}{\partial H}_0 & \frac{\partial t}{\partial \gamma}_0 \\ \frac{\partial \lambda_h}{\partial \lambda_h}_0 & \frac{\partial \lambda_h}{\partial H}_0 & \frac{\partial \lambda_h}{\partial \gamma}_0 \end{bmatrix} = \begin{bmatrix} \frac{\partial V}{\partial \lambda_h}_0 & \frac{\partial V}{\partial H}_0 & \frac{\partial V}{\partial \gamma}_0 \\ \frac{\partial t}{\partial \lambda_h}_0 & \frac{\partial t}{\partial H}_0 & \frac{\partial t}{\partial \gamma}_0 \\ 1 & 0 & 0 \end{bmatrix} \qquad (64)$$

Note that time appears in this problem as a state-like variable with

$$t' = \frac{1}{V\text{Cos}\gamma} \qquad (65)$$

A prime on the variables denote differentiation with respect to the range variable x.

From (64), the sign of

$$\frac{\partial V}{\partial \gamma}_0 \cdot \frac{\partial t}{\partial H}_0 - \frac{\partial V}{\partial H}_0 \cdot \frac{\partial t}{\partial \gamma}_0 \qquad (66)$$

evaluated along the Euler solution determines the rank of the matrix (64). If the sign changes at any point on the trange trajectory it is indicative of a conjugate [illegible].

The Euler solution obtained for the time-range problem, with altitude dependence of μ suppressed, may now be tested for conjugate points. In view of the particularly simple form of the conjugate-point-test for this problem, it seems reasonable to attempt to obtain analytical approximations for the partial derivatives in (66).

Linearizing the equations of motion and the Euler equation (17) with range as the independent variable about an equilibrium point at a particular altitude,

$$\delta V' = a_0\,\delta V - a_1\,\delta\gamma \tag{67}$$

$$\delta t' = -a_2\,\delta V + a_3\,\delta\gamma \tag{68}$$

$$\delta\gamma' = a_4\,\delta V - a_5\delta\gamma + a_6\,\delta H \tag{69}$$

Where :

$$a_0 = \frac{g}{WV\cos\gamma}\,\frac{\partial}{\partial V}(T-D) \tag{70}$$

$$a_1 = \frac{g}{V} \tag{71}$$

$$a_2 = \frac{1}{V^2\cos\gamma} \tag{72}$$

$$a_3 = \frac{\sin\gamma}{V\cos^2\gamma}$$

$$a_4 = -\frac{\cos\gamma\, g}{V^4}\,\frac{H}{\lambda_x} + \frac{\partial(T-D)}{\partial V}\,\frac{g}{V^2(T-D)}\left[1 - \frac{\cos\gamma}{V}\,\frac{H}{\lambda_x}\right] + \frac{g}{V(T-D)^2}\left\{\frac{\partial(T-D)}{\partial V}\right\}^2\left[1 - \frac{\cos\gamma}{V}\,\frac{H}{\lambda_x}\right] + \frac{g}{V(T-D)}\,\frac{\partial^2(T-D)}{\partial V^2}\left[\frac{\cos\gamma}{V}\,\frac{H}{\lambda_x} - 1\right] \tag{73}$$

$$a_5 = a_0 \tag{74}$$

$$a_6 = \frac{\cos\gamma}{V^3(T-D)}\,\frac{g}{\lambda_x}\left[V\,\frac{\partial(T-D)}{\partial V} + (T-D)\right] \tag{75}$$

Equations (67), (68) and (69) constitute a linear, constant-coefficient system which can be put in the following form using Laplace transforms (initial conditions on δV and δt are zero)

$$\frac{\delta V(s)}{\delta\gamma(0)} = \frac{-a_1}{s^2+(a_1a_4-a_0a_5)} \tag{76}$$

$$\frac{\delta V(s)}{\delta H(0)} = \frac{-a_1a_6}{s\left[s^2+(a_1a_4-a_0a_5)\right]} \tag{77}$$

$$\frac{\delta t(s)}{\delta\gamma(0)} = \frac{-\left[(a_0a_3-a_1a_2)-a_3s\right]}{s\left[s^2+(a_1a_4-a_0a_5)\right]} \tag{78}$$

$$\frac{\delta t(s)}{\delta H(s)} = \frac{-\left[(a_0a_3-a_1a_2)-a_3s\right]a_6}{s^2\left[s^2+(a_1a_4-a_0a_5)\right]} \tag{79}$$

putting $\omega_n^2 = (a_1a_4-a_0a_5)$ (80)

and

$$T = \frac{-a_3}{a_0a_3-a_1a_2} \tag{81}$$

and cancelling out common constants in the numerator, the equations (76) - (79) can be brought to the form

$$\frac{\delta V(s)}{\delta\gamma(0)} = \frac{\omega_n^2}{s^2+\omega_n^2} \tag{82}$$

$$\frac{\delta V(s)}{\delta H(0)} = \frac{\omega_n^2}{s(s^2+\omega_n^2)} \tag{83}$$

$$\frac{\delta t(s)}{\delta\gamma(0)} = \frac{(1+Ts)\omega_n^2}{s(s^2+\omega_n^2)} \tag{84}$$

$$\frac{\delta t(s)}{\delta H(0)} = \frac{(1+Ts)\omega_n^2}{s^2(s^2+\omega_n^2)} \tag{85}$$

Equations (84) and (85) may be further simplified using the expression (82) and (83).

$$\frac{\delta t(s)}{\delta\gamma(0)} = \frac{\delta V(s)}{\delta H(0)} + T\,\frac{\delta V(s)}{\delta\gamma(0)} \tag{86}$$

$$\frac{\delta t(s)}{\delta H(0)} = \frac{\omega_n^2}{s^2(s^2+\omega_n^2)} + T\,\frac{\delta V(s)}{\delta H(0)} \tag{87}$$

Equations (86) and (87) imply

$$\frac{\delta t(x)}{\delta\gamma_0} = \frac{\delta V(x)}{\delta H_0} + T\,\frac{\delta V(x)}{\delta\gamma_0} \tag{88}$$

$$\frac{\delta t(x)}{\delta H_0} = L^{-1}\left[\frac{\omega_n^2}{(s^2+\omega_n^2)s^2}\right] + T\,\frac{\delta V(x)}{\delta H_0} \tag{89}$$

using (88) and (89) in (66)

$$\frac{\partial V}{\partial\gamma_0}\cdot\frac{\partial t}{\partial H_0} - \frac{\partial V}{\partial H_0}\cdot\frac{\partial t}{\partial\gamma_0} = \frac{\delta V(x)}{\delta\gamma_0}L^{-1}\left[\frac{\omega_n^2}{s^2(s^2+\omega_n^2)}\right] - \left\{\frac{\delta V(x)}{\delta H_0}\right\}^2 \tag{90}$$

And consequently, one needs to obtain the inverse transform of only three transfer functions, namely

$$\frac{\delta V(s)}{\delta\gamma_0}\ ,\ \frac{\delta V(s)}{\delta H(0)}\ ,\ \frac{\omega_n^2}{s^2(s^2+\omega_n^2)}$$

when ω_n^2 is positive, the roots of the denominator polynomial are conjugates and

$$\frac{\partial V}{\partial\gamma_0}\cdot\frac{\partial t}{\partial H_0} - \frac{\partial V}{\partial H_0}\,\frac{\partial t}{\partial\gamma_0} = \omega_n x\sin(\omega_n x) + 2\cos(\omega_n x) - 2 \tag{91}$$

The right hand side of (91), after being zero at $x = 0$, will subsequently become zero at

$$x = \frac{2\pi}{\omega_n} \tag{92}$$

implying that conjugate points will occur every full cycle of oscillatory solution. Hence, if the

equilibrium point for the given H/λ_X is stable, i.e. it produces an oscillatory solution, a conjugate point will occur at the end of one full cycle of the oscillation. On the other hand, if w_n^2 is negative, the roots are real and distinct, symmetric about the imaginary axis. In this case

$$\frac{\partial V}{\partial \gamma_0} \cdot \frac{\partial t}{\partial H_0} - \frac{\partial V}{\partial H_0} \frac{\partial t}{\partial \gamma_0} \neq \tag{93}$$

$$-x.d.\text{Sinh}(dx) + 2\,\text{Cosh}(dx) - 2$$

Where $d = \sqrt{|\omega_n^2|}$

Expression (93) is zero only at $x = 0$. In this case, conjugate points do not occur. From (93), then, if the equilibrium point for the given H/λ_X is unstable, conjugate points will not occur.

The conjugate-point test is now applied to the three regimes of H/λ_X described earlier. As expected, for all values of H/λ_X to the left of V(T-D) max point, conjugate points occur, indicating that the Euler solutions obtained with these values of H/λ_X do not afford a maximum to the time-range problem over long intervals. Euler solutions obtained with $H/\lambda x$ to the right of the $V(T-D)_{max}$ point, on the other hand, satisfy the Legendre-Clebsch necessary conditions and Jacobi's necessary condition, and hence are optimal trajectories for the time-range problem.

Numerical solution of the time-range problem:

With the insight gained for the time-range problem with altitude dependence of thrust and drag suppressed, we now embark upon a numerical study of the more general case in which the aerodynamic coefficients are functions of Mach number and the thrust is Mach-altitude dependent. The data for a version of the F-4 aircraft with afterburner operative are used in this study. A cubic-spline representation (Ref. 10) is used to compute the values of zero-lift drag coefficient and the induced-drag coefficient. The drag coefficient is then computed as

$$C_D = C_{D_0}(M) + K(M)\, C_L^2$$

Where $C_L = \frac{W}{\frac{1}{2}\rho V^2 S}$ and C_{D_0} and K are standard notation.

The drag is then obtained as the usual product of drag coefficient, dynamic pressure and the aircraft wing area. A cubic-spline lattice (Ref. 10) is used to compute the value of thrust at a given altitude and Mach number. Atmosphere density and speed of sound as functions of altitude are interpolated from standard atmosphere tables using cubic splines. The system differential equations are integrated using a fifth-order Runge-Kutta-Verner method with variable step size.

A plot of H/λ_X vs airspeed for equilibrium flight conditions corresponding to unaccelerated flight with specific energy $E = h + \frac{V^2}{2g}$, frozen at 60,000' is shown in Fig. 9. The three regimes of H/λ_X identified earlier in this paper can be seen in Fig. 9. Numerical integration of the Euler equation with H/λ_X values picked from each of these regimes indicated that the solution for H/λ_X values to the left of $V(T-D)_{max}$ are oscillatory. Numerical solution using H/λ_X to the right of $V(T-D)_{max}$ point (high speed end) are non oscillatory and violent in character.

Next, a numerical conjugate-point test is set up based on a scheme suggested by Cicala (Ref. 11). In this scheme the partial derivatives with respect to λ_{i_0} required in the matrix (64) are calculated approximately in terms of difference quotients. Small increments in initial λ_i are employed in the evaluation of neighboring solutions of the original system of Euler equation. The conjugate-point test was carried out for various values of H/λ_X picked from Fig. 9. It was found as expected that only the non-oscillatory trajectories corresponding to H/λ_X values on the right of $V(T-D)_{max}$ satisfy the no conjugate point condition. Oscillatory trajectories indicate the existence of a conjugate point after a cycle of oscillation.

From the foregoing it is clear that the solution to time-range optimal-control problems are nonoscillatory and violently unstable in character. Within the permissible range of H/λ_X, as H/λ_X increases, the Euler solutions approach the energy climb schedule in the V,h plane. Of particular interest in practical applications is that trajectory which terminates at the "dash-point" on the flight envelope, the maximum-level-flight-speed point. To determine the value of H/λ_X which will accomplish this, a plot of the locus of equilibrium points corresponding to unaccelerated flight at constant energy is made. Once this value H/λ_X is found, what remains to obtain the optimal trajectory is to determine the initial value of the control variable γ for a given set of initial conditions on altitude and airspeed.

In Fig. 10 the level-flight envelope for the F-4 aircraft is shown along with the energy-climb schedule. The discontinuity in the energy-climb schedule due to transonic drag rise may be noted (Ref. 12). The curve B is the locus of equilibrium points at each energy level corresponding to unaccelerated flight with the appropriate H/λ_X. The discontinuity due to transonic drag rise is again visible. An Euler solution for initial values of airspeed and altitude close to the equilibrium locus is also shown. To determine this trajectory an iteration was undertaken on the initial value of the control variable γ. With quadruple precision on the IBM-370/158, the initial path angle had to be determined to 13 significant digits. To illustrate the sensitivity of the Euler solution to the initial value of path angle γ, the last digit of γ_0 is perturbed in the positive and negative sense with the trajectories 1 and 2 shown in Fig. 10 resulting.

A few more Euler solutions with initial conditions far removed from the equilibrium locus are shown in Fig. 11.

Discussions and Conclusions:

In this paper, optimal flight in the vertical plane with a vehicle model intermediate in complexity between point-mass and energy models was studied. Flight path angle takes on the role of control variable in the model and range-open problems feature subarcs of vertical flight and singular subarcs as previously studied.

Minimum-range climb problem (the steepest climb of Ref. 15) has been found to have no minimum, not even a lower bound. In reference 15, the steepest-climb problem was studied using the Green's theorem device of reference 13 and 14. There is an important difference in vehicle modelling from that of the present paper which should be noted as a key to resolving disparities between the character of optimal paths emerging. The analysis of Ref. 13 and 15 in essence replace $\cos\gamma$ in equation (3) with unity so that the problem solved is maximum altitude in a given distance (i.e. arc length) rather than in a given range. This is a necessity with the linear-integral approach which can accomodate only problems of dimension two and very special form of state equations. The solution to the distance climb consists of a central path flown along a $(T-D)_{max}$ locus in the V-h plane with vertical climb and dive transitions at the ends to meet specified boundary conditions.

From physical considerations it can be seen that when a positive margin of thrust over drag exists, the maximum-range climb trajectory without time or fuel constraints has no proper maximum nor an upper bound. In view of this fact major attention has been accorded to the time-range problem.

For the special case in which the thrust and drag depend only on airspeed, a plot of the ratio of time and range multipliers H/λ_x for equilibrium, corresponding to unaccelerated flight, revealed the existence of three regimes. Positive values of H/λ_x on the low-speed side of $V(T-D)_{max}$ and all negative values of H/λ_x were shown to yield oscillatory solutions. Although these meet the Legendre-Clebsch necessary conditions, they fail the conjugate-point test. Euler solutions with H/λ_x chosen to the right of the $V(T-D)_{max}$ point satisfy both Legendre-Clebsch and Jacobi necessary conditions and are nonoscillatory in character. Depending on the nature of aircraft data, unstable equilibrium points may sometimes appear for certain H/λ_x values to the left of airspeed corresponding to $(T-D)_{max}$ at certain energy levels. These normally have short duration and are not of major interest.

Numerical solution of the Euler equation and a numerical conjugate-point test for the F-4 aircraft data reinforced the conclusions arrived at in the analytical exercise.

From a practical viewpoint, the time-range trajectories which terminate at the "dash-point" on the level flight envelope are of particular interest. The multiplier ratio H/λ_x corresponding to this point is determined using the locus of equilibrium points at each energy level corresponding to unaccelerated flight. With this value of H/λ_x, Euler solution for any (h,V) pair is obtained by iterating on the initial value of γ, the control variable.

Euler solutions were obtained for various initial conditions. One observes that these tend to funnel rapidly into a certain corridor in the V-h chart, in the vicinity of the equilibrium locus corresponding to unaccelerated flight. This feature of the solution family can be exploited in practical situations to simplify the computation of optimal trajectories.

References:

1. Kaiser, F.; Der Steigflug mit Strahlflugzeugen-Tiel 1, Bahngeschwindigkeit Für Besten Steigens, Versuchsbericht 262-02-L44, Messerschmitt A. G., Augsburg, April 1944. (Translated as Ministry of supply RTP/TIB translation GDC/15/148T).

2. Lush, K. J.; A review of the problem of choosing a climb technique with proposals for a new climb technique for high performance aircraft, Aeronautical Research Council Report Memo, No. 2557, 1951.

3. Rutowski, E. S.; Energy approach to the general aircraft performance problem, Journal of the Aeronautical Sciences, Vol. 21, No. 3, March 1954.

4. Kelley, H. J.; Cliff, E. M. and Weston, A. R., Energy State Revisited, in preparation.

5. Kelley, H. J.; An investigation by variational methods of flight paths for optimum performance, Sc.D. Dissertation , New York University, May 1958.

6. Kamke, E.; Differentialgleichungen, Lösungmethoden und Lösungen, Band 1, Gewöhnliche Differentialgleichungen, Third edition, Chelsea publishing Co., New York, N. Y., 1948.

7. Boyce, W. E. and Diprima, R. C.; Elementary Differential equations and Boundary Value Problems, Third edition, John Wiley and Sons, New York, N. Y., 1977.

8. Weston, A. R.; On-board Near-optimal Climb-Dash Energy Management, Ph.D. Dissertation, Virginia Polytechnic Institute and State University, December 1982.

9. Kelley, H. J. and Moyer, G. H.; Jacobi's Necessary Conditions, in Topics in Optimization Theory, Grumman Research Department Report RE-159, June 1962.

10. Mummolo, F. and Lefton, L.; Cubic Splines and Cubic-Spline Lattices for Digital Computation, Analytical Mechanics Associates, Inc. Report No. 72-28, July 1972. Revision dated December 1974.

11. Cicala, P.; An Engineering Approach to Calculus of Variations, Levrotto-Bella, Torino, Italy, 1957.

12. Weston, A. R., Cliff, E. M. and Kelley, H. J.; Altitude Transitions in Energy Climbs, AUTOMATICA, Vol. 19, No. 2, March 1983.

13. Miele, A.; Problemi di Minimo Tempo Nel Volo Non-stazionario degli Aeroplani, Atti della Accademia delle scienze di Torino, Vol. 85, 1950-51, pp. 41-42.

14. Mancill, J. D.; Identically non-regular problems in the calculus of variations, Mathematica Y Fisica Teorica, Vol. 7, No. 2, June 1950; Tucuman, Argentina.

15. Miele, A.; General Solutions of Optimum Problems in Nonstationary Flight, NACA TM-1388, October 1955.

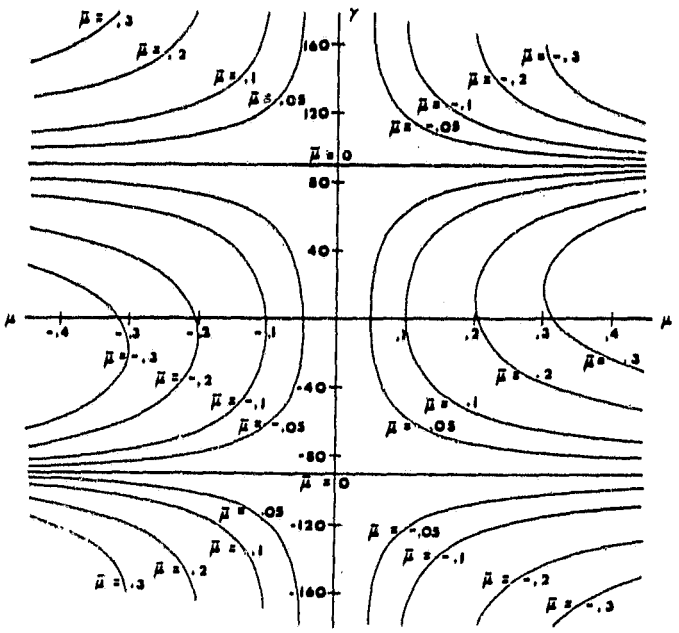

Fig. 1 . Path Angle vs. Power Variable for Range Problem

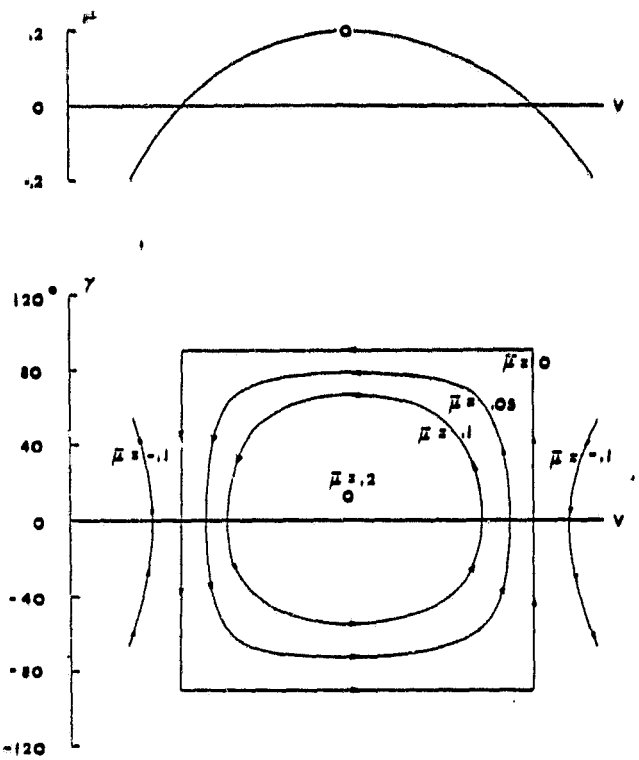

Fig. 3 . Path Angle vs. Airspeed in Powered Flight for Range Problem

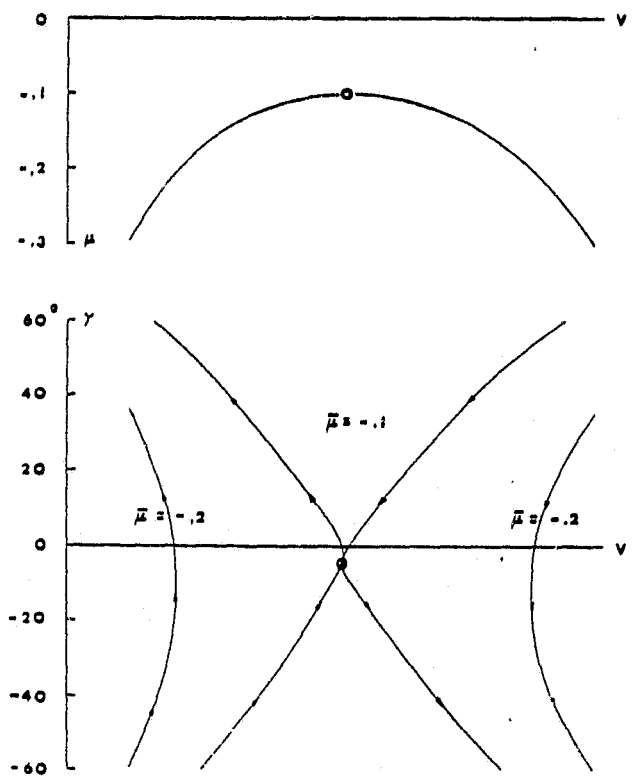

Fig. 2 . Path Angle vs. Airspeed in Gliding Flight for Range Problem

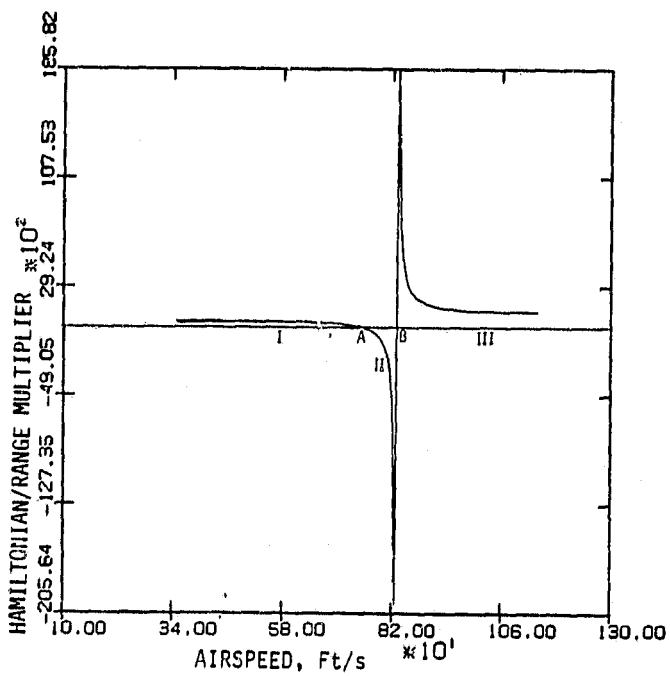

Fig. 4 . H/λ_x vs. Airspeed at Equilibrium points
(Parabolic (T-D)/W distribution)

A: $(T-D)_{max}$

B: $V(T-D)_{max}$

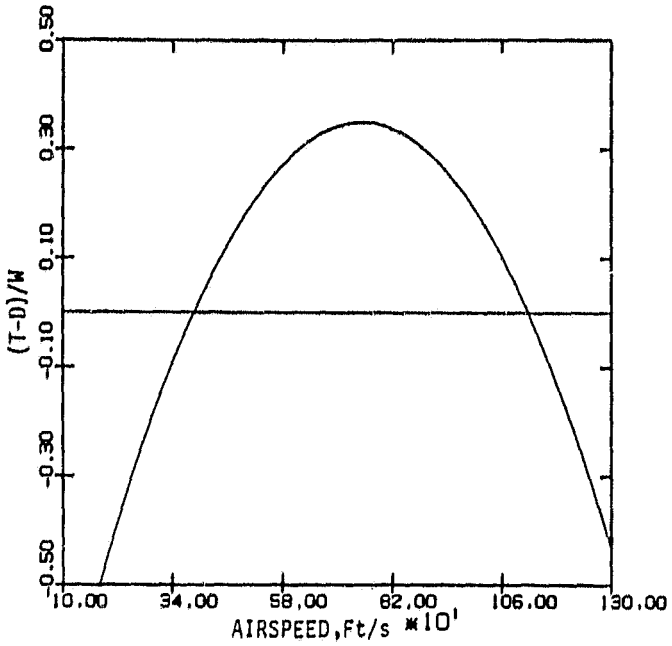

Fig. 5 . (T-D)/W vs. Airspeed - A typical Parabolic distribution

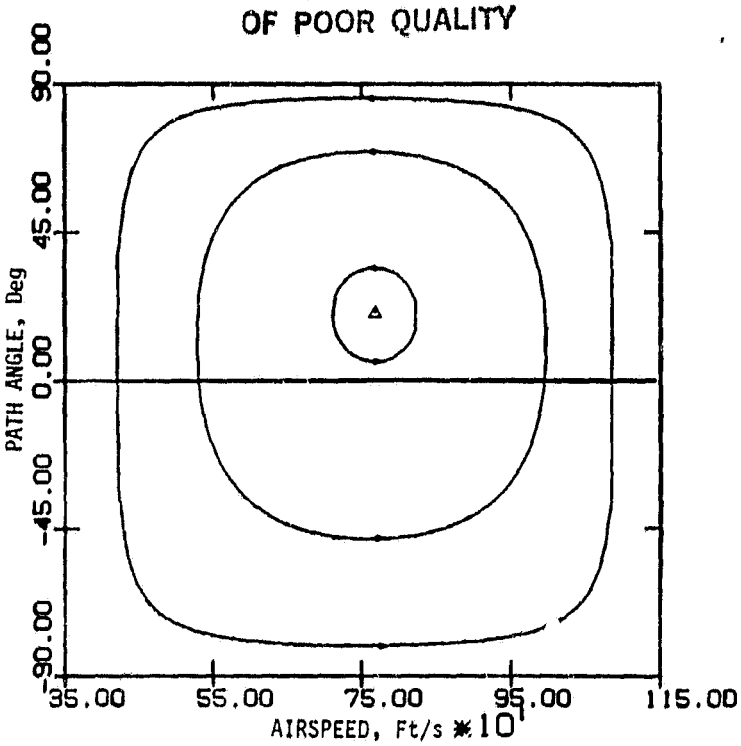

Fig. 7 . Representative Analytical Solution for H/λ_x in the Second Equilibrium Regime

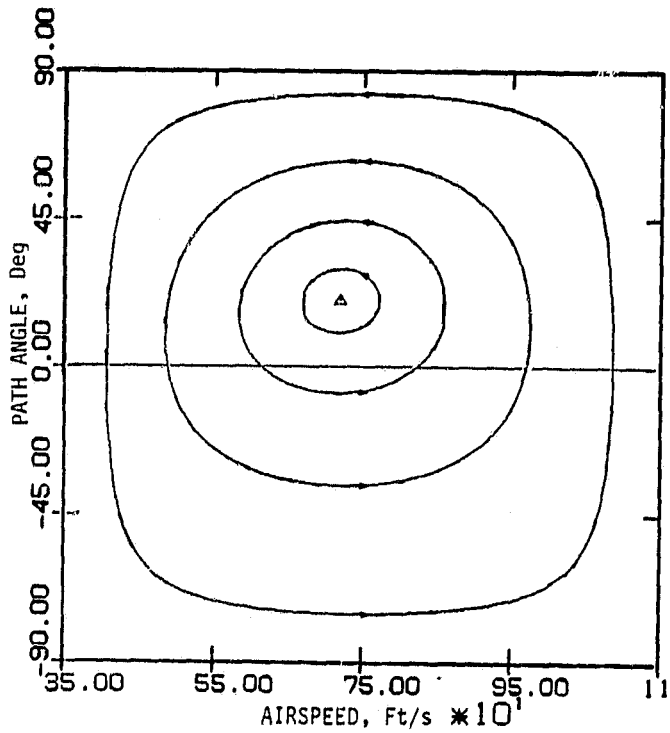

Fig. 6 . Representative Analytical Solution for H/λ_x in the First Equilibrium Regime

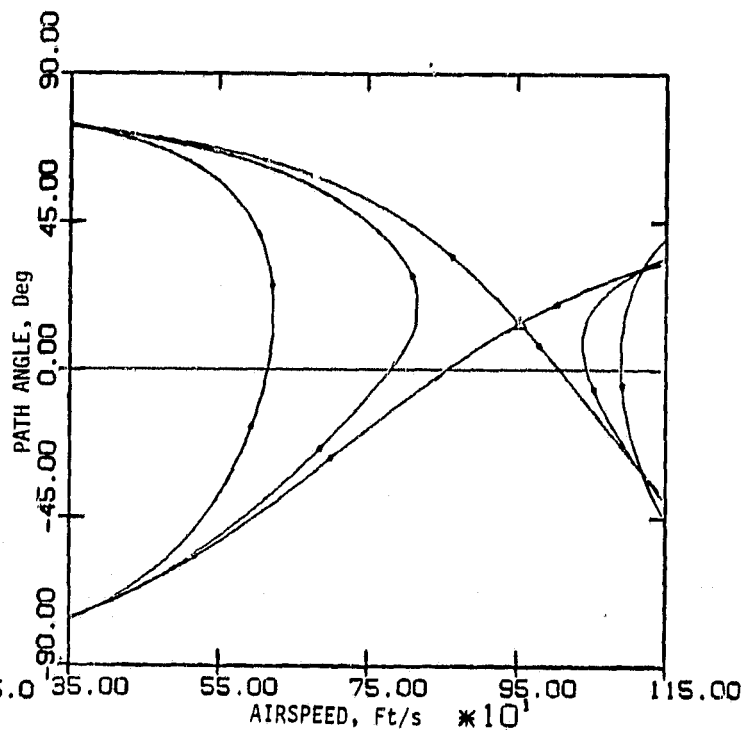

Fig. 8 . Representative Analytical Solution for H/λ_x in the Third Equilibrium Regime

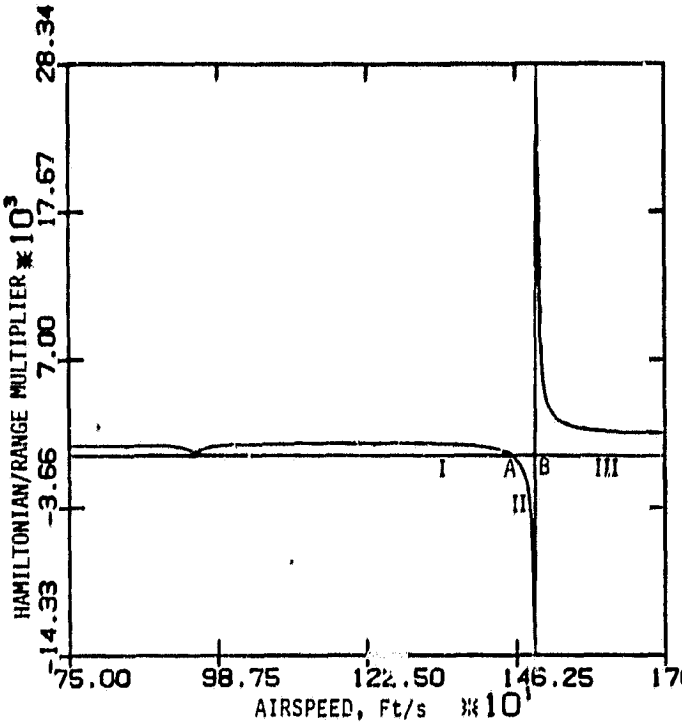

Fig. 9 . H/λ_x vs. Airspeed at Constant Specific Energy for F-4 Aircraft for Unaccelerated Flight

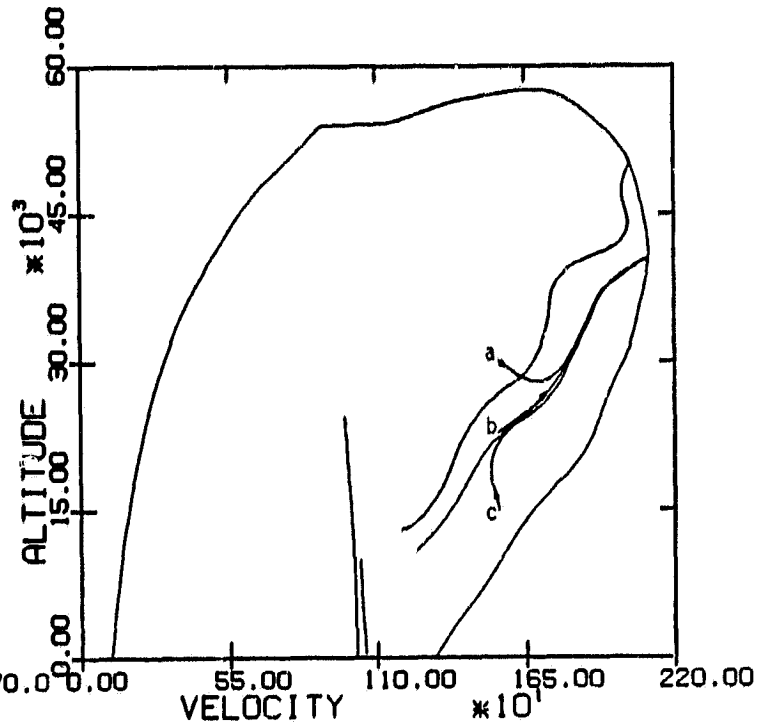

Fig. 11 . Euler Solutions for the Fixed Time - Range Maximization Problem
a, b, c: Euler Solutions

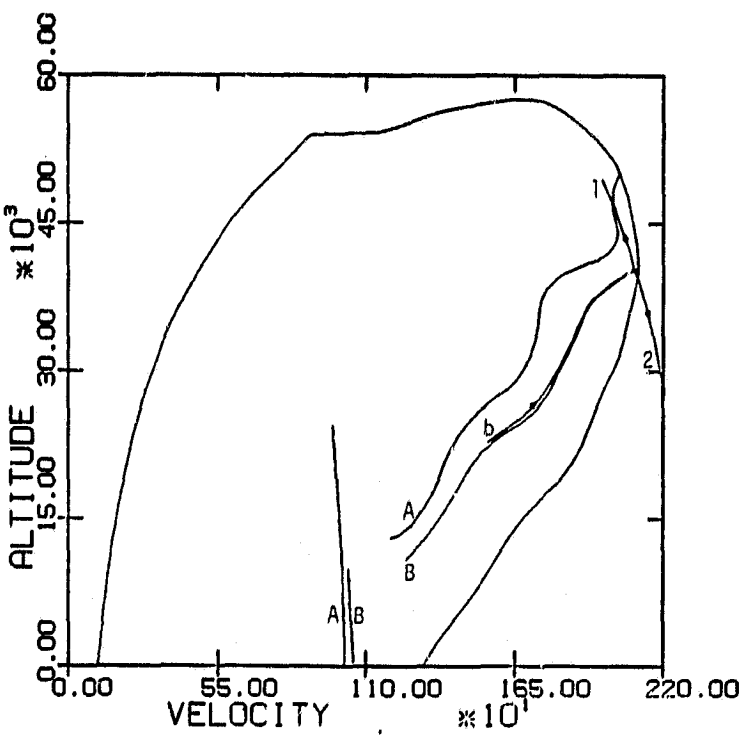

Fig. 10 . Flight Envelope, Energy Climb Schedule, Equilibrium Locus and the Euler Solution
A: Energy Climb Schedule
B: $\dot{\gamma} = 0$ Locus
b: Euler Solution

ENERGY STATE REVISITED

Henry J. Kelley
Eugene M. Cliff
Alan R. Weston
Virginia Polytechnic Institute and State University
Blacksburg, Virginia

Abstract

Minimum-time climbs in "energy" approximations are reviewed and further consideration given to choice of variables. A pair of variables which seem to offer attractive replacements for altitude and airspeed in singular-perturbation procedures is suggested. Use of the new variables in an energy-modelled climb-dash problem is illustrated.

Introduction

In Ref. 1, Fritz Kaiser, a flight-test engineer at Messerschmitt, A. G., introduced the concept of "GESAMTHÖHE" ("resultant height") in connection with aircraft minimum-time climbs. This is the sum of potential and kinetic energy per unit weight. Subsequently it has been referred to as "energy height"[2,3] and "specific energy".[4] Its use as a state variable in trajectory work is attractive because it is a "slower" variable than either altitude or velocity.[5,6,7] Attempts to synthesize "slow" state variables are described in Refs. 6 and 7 in connection with singular-perturbation procedures. The present development attempts to synthesize both "fast" and "slow" variables for the minimum-time-to-climb problem along lines explored earlier in an appendix to Ref. 6.

Climb Equations

The equations of motion for climbing flight are given in terms of conventional state variables, altitude, h, flight-path angle, γ, and velocity, V, as

$$\dot{h} = V \sin\gamma \tag{1}$$

$$\dot{\gamma} = \frac{g}{V}\left(\frac{L}{W} - \cos\gamma\right) \tag{2}$$

$$\dot{V} = \frac{g(T-D)}{W} - g\sin\gamma \tag{3}$$

Here T is thrust, D drag, L lift and g the acceleration of gravity. An assumption of thrust-along-the-path has been incorporated.

Energy-Modelling Simplifications

An essential feature of "energy" approximation is that drag be treated as a function of h and V only. This is consistent with approximation of $\sin\gamma$ and $\cos\gamma$ via expansion in powers of γ through first-order terms only and with deletion of the $\dot{\gamma}$ term as negligible -- another feature essential to reduction in order. With these simplifications the system becomes

$$\dot{h} = V \tag{4}$$

$$\dot{V} = \frac{g(T-D)}{W} - g\gamma \tag{5}$$

where D(h,V) is evaluated for L = W.

"Slow"-Variable Choice

Two new variables, ϕ and ψ, are to be introduced in place of h and V, ϕ to be "slow" and ψ "fast".

The equation of state for ϕ is

$$\dot{\phi} = \frac{\partial\phi}{\partial h}\dot{h} + \frac{\partial\phi}{\partial V}\dot{V}$$

$$= \frac{\partial\phi}{\partial V}\left[\frac{g(T-D)}{W}\right] + \left[V\frac{\partial\phi}{\partial h} - g\frac{\partial\phi}{\partial V}\right]\gamma \tag{6}$$

If one insists that $\dot{\phi}$ be independent of the control-like variable, γ, then ϕ must satisfy the partial differential equation

$$V\frac{\partial\phi}{\partial h} - g\frac{\partial\phi}{\partial V} = 0 \tag{7}$$

This is satisfied by

$$\phi = h + \frac{V^2}{2g} \tag{8}$$

or by any once-differentiable function of this expression.[6] Thus $\phi = E$, specific energy, is "slow" in the sense specified.

"Fast"-Variable-Choice Considerations

It has been usual to adopt as the second state variable, ψ, either V[5] or h.[7] Either is suitable for analysis of the "slow" motion, given by the single state equation

$$\dot{E} = \frac{V(T-D)}{W} \tag{9}$$

For minimum-time passage to higher energy levels, the right member of (9) is maximized with respect to V or h at constant E. The expression on the right of (7) is "specific excess power", P_s, of the flight-performance literature (e.g. Ref. 4) and simply p later in the present paper. With a more general choice of $\psi(V,h)$, the maximization of (9) is done with respect to this variable after V and h have been replaced by suitable functions of ϕ and ψ representing the inverse transformation. The resulting values of V, h and $\dot{E}$ are the same, however.

Singular-Perturbation Analysis

The choice of $\psi(V,h)$ matters, however, in the determination of γ along the "slow-motion" (or "outer") solution, as γ must be such that $\dot{\psi} = 0$, in the procedure of Ref. 7. With the choice of $\psi = h$ as in Ref. 7, the approximation $\gamma = 0$ is obtained, while if $\psi = V$ is assumed, then

$$\gamma = \frac{(T-D)}{W} \tag{10}$$

which is, to linear approximation in γ, the path angle for unaccelerated climb. More generally the expression

$$\dot{\psi} = \frac{\partial \psi}{\partial h}\dot{h} + \frac{\partial \psi}{\partial V}\dot{V}$$

$$= \frac{\partial \psi}{\partial h} V\gamma + \frac{\partial \psi}{\partial V}\left[\frac{g(T-D)}{W} - g\gamma\right] = 0 \tag{11}$$

is to be solved to obtain the zeroth-order "outer" approximation for γ. The choice

$$\psi = \left.\frac{\partial p}{\partial h}\right|_E \tag{12}$$

suggests itself for compatibility with the outer solution, for

$$\dot{\psi} = \frac{\partial \psi}{\partial h} V\gamma + \frac{\partial \psi}{\partial V}\left[\frac{g(T-D)}{W} - g\gamma\right] \tag{13}$$

Here

$$p \equiv \frac{V(T-D)}{W} \tag{14}$$

is "specific excess power," a known function of h and V. This choice of ψ is seen to generate zeroth-order γ consistent with (4) and (5) along the outer solution.

Choice of "Fast" Variable

Contours $\phi = E = \text{const.}$ and $\psi = \text{const.}$ are shown in Fig. 1 for the aircraft data of Ref. 9 (a version of the F-4). The contours of $\psi = \text{constant}$ indicate a breakdown of one-to-one mapping associated with jumps of the energy-climb path, $\psi = 0$, between ridges of $p(h,V)$[9]; in fact, the mapping $\phi,\psi \to h, V$ is two-to-one and even three-to-one within the flight envelope. This local non-invertibility represents a less-than-ideal feature for a coordinate transformation; however, one does not actually have to transform to the new variables to exploit the concept.

Flight-path angle γ is shown as a function of $\phi = E$ in Fig. 2 for three choices of "fast" variable: h, V and ψ. The contribution of the "outer" solution (shown) dominates the zeroth-order composite solution. Experience is that the calculation of first- and higher-order composites is intricate and expensive.[10] Thus it makes sense to choose variables carefully so as to enhance the fidelity of the zeroth-order solution as far as possible.

Climb-Dash Problem

Consider as an application the climb-dash problem, in which a minimum-time trajectory to a remote value of x is sought, where x is down-range and, for small γ is defined by

$$\dot{x} = V \tag{15}$$

The character of the solution is that of a combined climb-dash generally faster than an energy climb (Fig. 3) fairing into sustained flight at the high-speed point on the level-flight envelope. γ as a function of E is shown in Fig. 4 for the three choices of fast variable. Solutions of a corresponding point-mass-modelled problem for different aircraft data are studied in Ref. 8.

Acknowledgments

The writers wish to thank David Hull and Jason Speyer of the University of Texas, Austin, for stimulating discussions. Thanks are also due to Philip Reed of the Imperial War Museum, London, and Wolfgang Herbst of MBB Fluzeuge, Munich, for supplying copies of the Kaiser report in English and German, respectively. The support of NASA Langley Research Center for the research under NASA grant NAG 1-203, Technical Monitors Douglas Price and Christopher Gracey, is gratefully acknowledged.

References

1. Kaiser, F., "Der Steigflug mit Strahlflugzeugen; Teilbericht 1: Bahnngeschwindigkeit für Besten Steigens," Versuchs-Bericht Nr. 262 02 L 44, Messerschmitt A.G., Lechfeld, May 1, 1944. Translated into English as R.T.P./T.I.B. Translation No. G.D.C./15/148T, Ministry of Supply (U.K.).
2. Lush, K. J., "A Review of the Problem of Choosing a Climb Technique with Proposals for a New Climb Technique for High-Performance Aircraft," Aeronautical Research Council Report Memorandum No. 2557, 1951.
3. Rutowski, E. S., "Energy Approach to the General Aircraft Performance Problem," Journal of the Aeronautical Sciences, Vol. 21, No. 3, March 1954.
4. Boyd, J. R., Christie, T. F., and Gibson, J. E., "Energy Maneuverability," Armament Laboratory Report, Vols. I and II, Eglin AFB, 1966.
5. Bryson, A. E., Desai, M. N., and Hoffman, W. C., "The Energy-State Approximation in Performance Optimization of Supersonic Aircraft," AIAA Journal, 1969.
6. Kelley, H. J., "State-Variable Selection and Singular Perturbations", in Singular Perturbations: Order Reduction in Control System Design, P. V. Kokotovic and W. R. Perkins, Editors, ASME, June 1972.
7. Kelley, H. J., "Aircraft Maneuver Optimization by Reduced-Order Approximation," in Control and Dynamic Systems, Volume 10, C. T. Leondes, Editor, Academic Press, 1973.
8. Weston, A. R., Cliff, E. M. and Kelley, H. J., "On-Board Near-Optimal Climb-Dash Energy Management," American Control Conference, San Francisco, California, June 22-24, 1982.

9. Weston, A. R., Cliff, E. M. and Kelley, H. J., "Altitude Transitions in Energy Climbs," AUTOMATICA, March 1983.
10. Ardema, M. D., "Solution of the Minimum-Time-to-Climb by Matched Asymptotic Expansions," AIAA Journal, July 1976.

Fig.1 Contours in the Altitude – Airspeed Chart

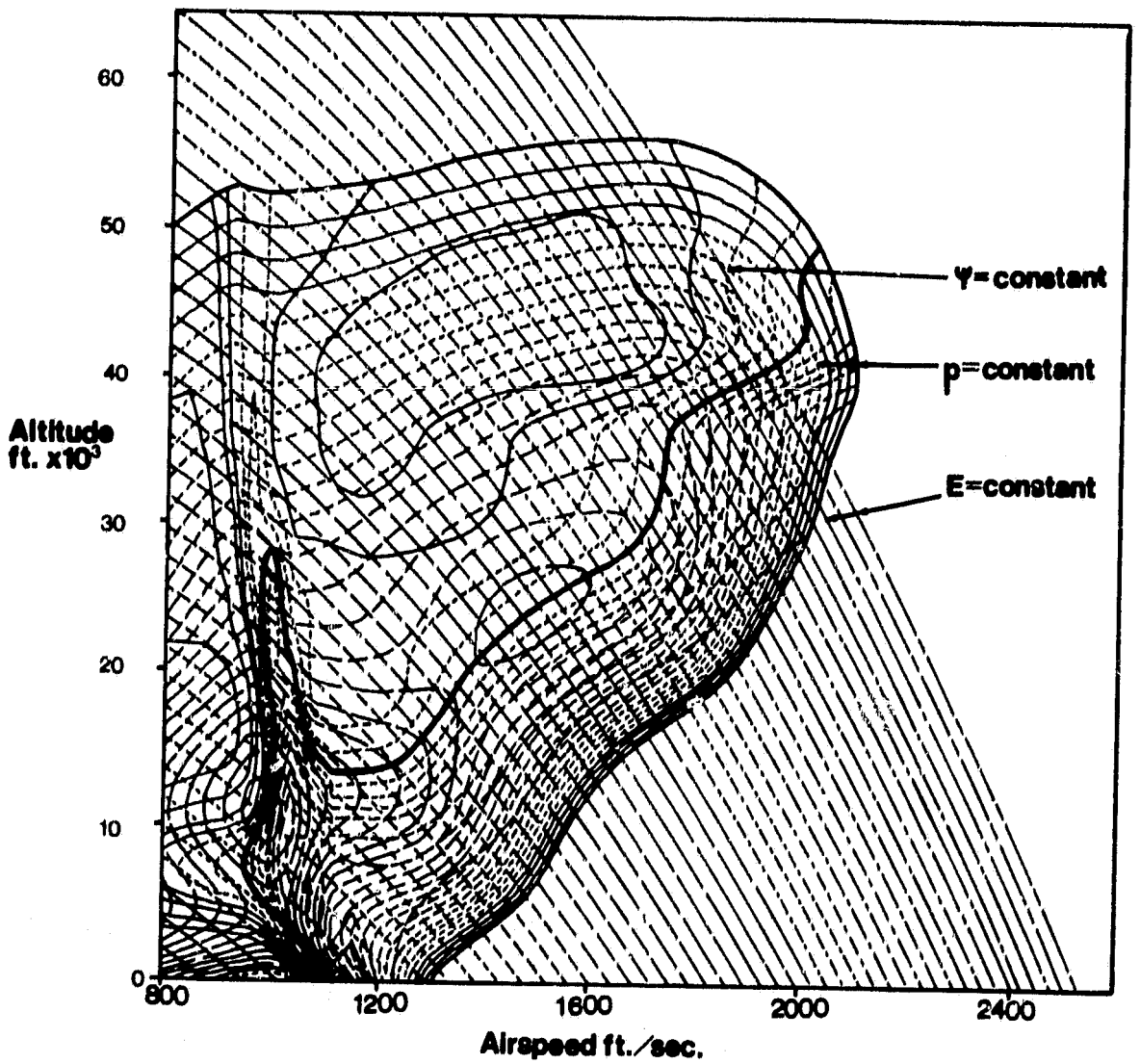

Fig.2 γ vs. E – Energy Climb

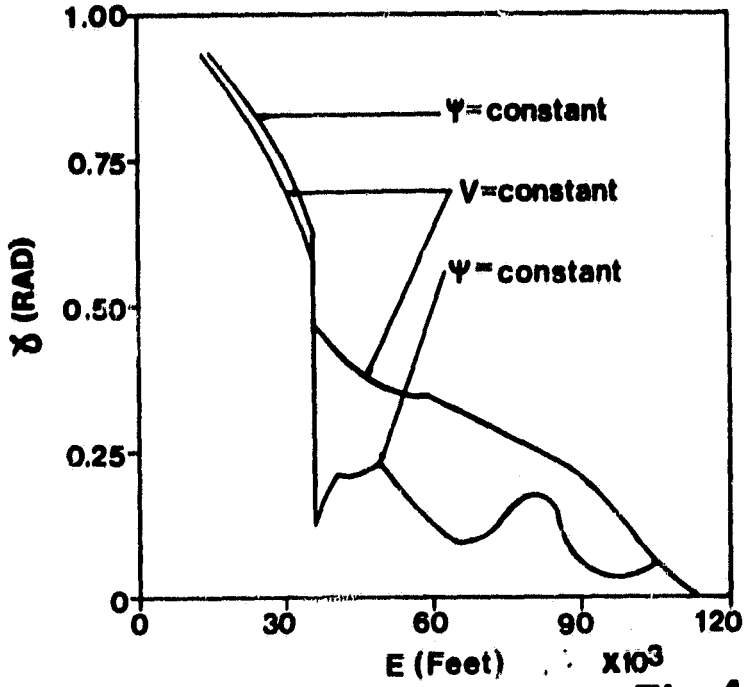

Fig.4 γ vs. E – Climb-Dash

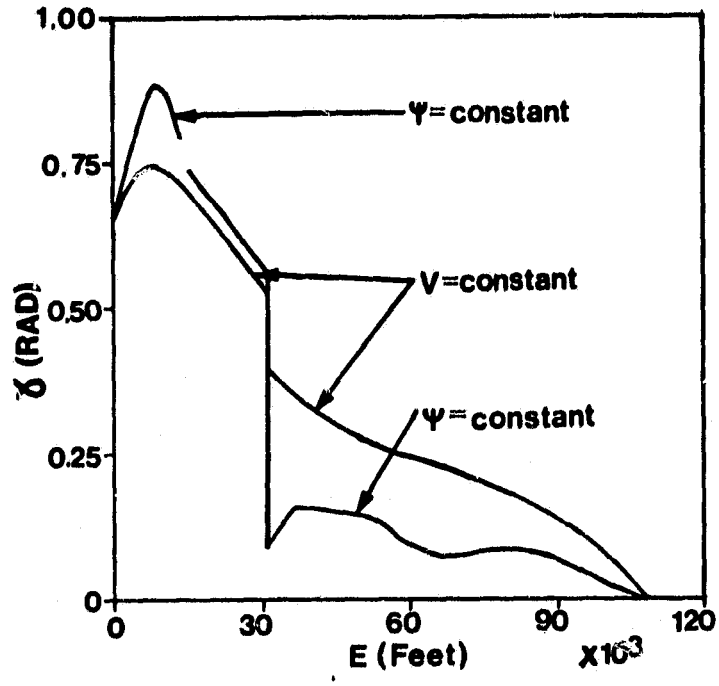

Fig.3 Altitude vs. Velocity - Climb - Dash